Beta-beams

Cristina Volpe†

† Institut de Physique Nucléaire Orsay, F-91406 Orsay cedex

Abstract.   Neutrino physics is traversing an exciting period, after the important discovery that neutrinos are massive particles, that has implications from high-energy physics to cosmology. A new method for the production of intense and pure neutrino beams has been proposed recently: the "beta-beam". It exploits boosted radioactive ions decaying through beta-decay. This novel concept has been the starting point for a new possible future facility. Its main goal is to address the crucial issue of the existence of CP violation in the lepton sector. Here we review the status and the recent developments with beta-beams. We discuss the original, the medium and high-energy scenarios as well as mono-chromatic neutrino beams produced through ion electron-capture. The issue of the degeneracies is mentioned. An overview of low energy beta-beams is also presented. These beams can be used to perform experiments of interest for nuclear structure, for the study of fundamental interactions and for nuclear astrophysics.

Contents

1. Introduction

The observations made by the Super-Kamiokande (Fukuda *et al* 1998), the K2K (Ahn *et al* 2003), the SNO (Ahmad *et al* 2001) and the KAMLAND (Eguchi *et al* 2003) experiments have brought a breakthrough in the field of neutrino physics. The longstanding puzzles of the *solar neutrino deficit*, observed by Davis' pioneering measurement (Davis 1964) and of the atmospheric anomaly have been clarified. We know now that the expected fluxes are reduced due to the neutrino oscillation phenomenon: the change in flavour that neutrinos undergo while traveling, first proposed by Pontecorvo (Pontecorvo 1957). An impressive progress has been achieved in our knowledge of neutrino properties, thanks to these experimental advances. Most of the parameters of the Maki-Nakagawa-Sakata-Pontecorvo (MNSP) unitary matrix, relating the neutrino flavor to the mass basis, are nowadays determined, except the third neutrino mixing angle, usually called θ_{13}. However, this matrix might be complex, meaning there might be additional phases – one Dirac and two Majorana phases, if neutrinos are Majorana particles. A non-zero Dirac phase introduces a difference between neutrino and anti-neutrino oscillations and implies the breaking of the $\mathcal{CP}$ symmetry in the lepton sector. On the other hand, the $\mathcal{CP}$ violating Majorana phases can manifest themselves in other processes like e.g. neutrinoless double-beta decay. The Majorana or Dirac nature of neutrinos, the value of the neutrino magnetic moment, the existence of sterile neutrinos, the neutrino mass scale (and hierarchy) and the possible existence of $\mathcal{CP}$ violation are among the crucial issues that remain open.

Neutrino oscillations imply that neutrinos are massive particles, contrary to what has been believed so far, and represent the first direct experimental evidence for physics beyond the Standard Model of elementary particles and interactions. Understanding the mechanism for generating the neutrino masses and their small values is clearly a fundamental question, that needs to be understood. On the other hand, the presently known (as well as unknown) neutrino properties have important implications for other domains of physics as well, among which astrophysics, e.g. for our comprehension of processes like the nucleosynthesis of heavy elements, and cosmology, for example for unraveling the asymmetry between matter and anti-matter in the Universe. Stars and the Universe constitute a precious laboratory for the study of the yet unknown neutrino properties, of fundamental interactions and for the search of new physics (Raffelt 1996). The present limits on the neutrino magnetic moment, on sterile neutrinos, or on the neutrino energy density coming from the cosmic microwave background and large scale structures (Bilenky *et al* 2003) are talkative examples of the strong constraints that can be extracted from the field of neutrino astronomy.

If the study of astrophysical and cosmological phenomena offers a unique way to progress on the open questions, performing terrestrial - accelerator and non-accelerator - experiments represent an irreplaceable procedure to obtain direct (model-independent) information. Many experiments, running, planned or under study, will bring invaluable results in the near future. In particular, the measurement of the third, less known,

neutrino mixing angle, as well as of the Dirac phase need the availability of very intense neutrino beams, and might require new methods besides conventional beams (coming from the decay of pions and muons) pushed to their ultimate intensities, or super-beams. The idea of a neutrino factory was first put forward, which is based on the production, collection, acceleration and storage of muons to obtain muon and electron (anti)neutrino beams. The neutrino energies are of several tens of GeV and the needed baseline of the order of 3000 Km. The aim is to address in one step the leptonic $\mathcal{CP}$ study, the neutrino hierarchy and the precise measurement of the θ_{23}, Δm_{23}^2 and θ_{13} oscillation parameters (Albright *et al* 2004).

Recently Zucchelli proposed the idea of producing electron (anti)neutrino beams using the beta-decay of boosted radioactive ions: the "beta-beam" (Zucchelli 2002). Such a novel concept has three main advantages: well-known fluxes, purity (in flavour) and collimation. This simple and attractive idea exploits major developments in the field of nuclear physics, where radioactive ion beam facilities, either planned or under study, are expected to reach ion intensities of 10^{11-13} per second. The main goals are to perform studies in the fields of nuclear structure, of fundamental interactions, in nuclear astrophysics, solid state physics, as well as for medical applications. Such intensities can render neutrino accelerator experiments using ions feasible as well, thanks to the beta-beam concept.

In the original scenario proposed by Zucchelli, the ions are produced, collected and accelerated first at several hundred MeV per nucleon, then at several tens GeV energies – after injection in the Proton Synchrotron (PS) and Super Proton Synchrotron (SPS) accelerators‡ – and finally stored in a storage ring of 7.5 km total length and of 2.5 km straight sections. This facility is based on reasonable extrapolation of existing technologies and exploits already existing accelerator infrastructure to reduce cost. The neutrino beam produced by the ions decaying along the straight sections point to a gigantic Čerenkov detector, located at the (upgraded) Fréjus Underground Laboratory, in order to study $\mathcal{CP}$ violation, through a comparison of $\nu_e \rightarrow \nu_\mu$ and $\bar{\nu}_e \rightarrow \bar{\nu}_\mu$ oscillations. A first feasibility study is performed in (Autin *et al* 2003) and discussed in (Lindroos 2003, Benedikt *et al* 2004). The discovery potential is now actively investigated (Mezzetto 2003, Bouchez *et al* 2003, Mezzetto 2005a, Mezzetto 2005b, Burguet-Castell *et al* 2004, Burguet-Castell *et al* 2005, Campagne *et al* 2006) and is also discussed in (Guglielmi *et al* 2005). Other technologies are also being considered for the detector, like liquid Argon Time Projection Chambers (Rubbia C 1977, Rubbia A 2004, Ereditato and Rubbia 2004 and 2005), nuclear calorimetry and emulsions.

The interest of the beta-beam concept for establishing a facility producing low-energy neutrino beams is soon recognized (Volpe 2004). Here the ions are accelerated at $\gamma = 5-14$ (γ is the Lorentz ion boost) to produce neutrino beams in the 100 MeV energy range. This idea opens new axis of research compared to the original scenario. Such beams can in fact be used for the study of nuclear structure, of fundamental interactions,

‡ Zucchelli considers CERN as a possible site for a beta-beam facility (Zucchelli 2002).

and of nuclear astrophysics. In particular, the physics potential covers experiments on spin-isospin and isospin nuclear excitations and neutrino-nucleus interactions (Volpe 2004, Serreau and Volpe 2004, McLaughlin 2004, Volpe 2005), measurements of the Weinberg angle (Balantekin *et al* 2006a), of the neutrino magnetic moment (McLaughlin and Volpe 2004) and CVC tests (Balantekin *et al* 2006b), or core-collapse Supernova physics (Volpe 2004, McLaughlin and Jachowitz 2006). A small devoted storage ring appears as more appropriate for these low energy applications (Serreau and Volpe 2004). Its feasibility study is now ongoing (Chancé and Payet 2005).

Other scenarios for the study of $\mathcal{CP}$ violation have been proposed afterwards, where the energy of the ions is much higher, the γ ranging from 150 (Burguet-Castell *et al* 2005) to several hundreds (medium energy) to thousands (high energy) (Burguet-Castell *et al* 2004). The value of 150 GeV per nucleon comes from the maximum acceleration that can be attained in the SPS. The baseline scenario in this case is the same as the original one. On the contrary, the medium and high energy options require major changes in the accelerator infrastructure, such as a refurbished SPS (or even the LHC) at CERN, as well as bigger storage rings. An increased distance between the source and the detector is also necessary to match the same oscillation frequencies. Therefore such scenarios imply further locations for the far detector, such as the Canfranc or the Gran Sasso Underground Laboratories. The physics potential is being actively investigated (Terranova *et al* 2004, Huber *et al* 2005, Agarwalla *et al* 2005, Donini *et al* 2005a) and is discussed in (Terranova 2004, Gomez-Cadenas 2005, Migliozzi 2005). It covers the third neutrino mixing angle, the $\mathcal{CP}$ violating phase, as well as the neutrino mass hierarchy. Some reduction of the degeneracy problem is also expected. This enlarged discovery potential is due to the information that can be extracted on the energy of the events; while in the original scenario the experiment is a counting measurement only. However, even if from the physics point of view pushing to higher energies appears as attractive, a specific and extensive feasibility study is needed, to determine in particular the ion intensities, that drastically influence the sensitivities, as well as the characteristics of the storage ring. From this point of view, the medium energy option appears as more promising, whereas the high energy one keeps at a much more speculative level.

The presence of degeneracies constitute an important open issue in the analysis of future accelerator neutrino experiments. This consists in the appearance of several disconnected regions in the oscillation parameter space, besides the true solutions. The origin of such regions is both the inherent three flavour structure of the oscillation probabilities, and some still unknown neutrino properties, namely the sign of Δm_{23}^2 and the octant of θ_{23}. The "fake" regions are usually referred to in the literature as the sign, the octant and the mixed degeneracies (or clones). They might render the identification of the true values of δ and θ_{13} more complex, depending on our knowledge of these unknowns at the time a beta-beam experiment takes place. Several possible strategies can be followed to resolve the problem of the clone solutions. An extensive analysis in the context of beta-beams is performed in (Donini *et al* 2004, Donini *et al* 2005b, Donini *et al* 2005c, Campagne *et al* 2006). An interesting and promising possibility is pointed

out in (Huber *et al* 2005c), i.e. to combine accelerator experiments with atmospheric data in the same detector.

Finally, monochromatic neutrino beams produced by boosted ions decaying through electron capture are proposed in (Bernabeu *et al* 2005a) and further discussed in (Bernabeu *et al* 2005b, 2005c and 2005d). The baseline envisaged here is the same as for the original beta-beam. In order to search for CP violation, instead of comparing neutrino versus anti-neutrino oscillations, a comparison of $\nu_e \rightarrow \nu_\mu$ oscillations (only ν_e are available) at different neutrino energies is necessary. Again, a specific feasibility study is needed in particular to state the ion rates at production and in the storage ring, since such a configuration requires the acceleration and storage of not fully stripped ions.

An attractive aspect of a beta-beam facility is that it offers strong synergies between different communities, to realize a multidisciplinary program covering hot open issues in various domains. In particular, the synergy between the nuclear and the neutrino physics communities has been quickly recognized. This has merged in a common feasibility study within the EURISOL Design Study, financed by the European Community in the FP6 Program (2005-2009), that is now ongoing. On the other hand the far detector can be used for other purposes, in particular, to measure neutrinos from a core-collapse Supernova explosion (in or outside our Galaxy), and to improve the present sensitivity on the proton decay. Finally, it is interesting to note that beta-beams can produce neutron beams as well, thanks to the beta-decay of boosted radioactive ions which emit delayed neutrons. This interesting possibility deserves further investigation.

Clearly the beta-beam concept has a broad physics potential, which explains why this field has been developing very fast since its very beginning, bringing many new ideas and scenarios. In this review we summarize the work done and try to give an overall view of the field. The review is meant not only for experts, but also as an introduction for non-experts. For this reason, many technical details are skipped, unless strictly necessary. From now on, unless stated differently, with the terminology "beta-beams" we refer to the original scenario. In Section I we recall the phenomenon of neutrino oscillations, the recent discoveries in neutrino physics, as well as how neutrino oscillations can be used to address the breaking of the $\mathcal{CP}, \mathcal{T}$ and $\mathcal{CPT}$ symmetries in the lepton sector. Section II presents the original beta-beam concept and baseline scenario, as proposed by Zucchelli, as well as the following sensitivity studies. In Section III low energy beta-beams and the physics potential discussed so far are presented. Section IV is devoted to the medium and high energy scenarios. The issue of the degeneracies is mentioned in Section V. Mono-chromatic neutrino beams based on electron capture are discussed in Section VI. Conclusions and perspectives are made in Section VII.

1.1. The neutrino oscillation phenomenon

Let us briefly remind the basic ingredients of neutrino oscillations. This phenomenon arises if neutrinos have masses and there is mixing. The evolution equation of the mass eigenstates in vacuum is simply $i(d/dt)|\nu_m\rangle = H_m|\nu_m\rangle$. This becomes $i(d/dt)|\nu_\alpha\rangle =$

$UH_mU^\dagger|\nu_\alpha\rangle$ in the flavor basis, where U is the unitary matrix which relates the weak ν_α ($\alpha = e, \mu, \tau$) to the mass ν_i ($i = 1, 2, 3$) eigenstates. Each flavour eigenstate can be written as $|\nu_\alpha\rangle = U_{\alpha i}|\nu_i\rangle$.

In general, a unitary $n \times n$ matrix depends on $n(n-1)/2$ angles and $n(n+1)/2$ phases. In the Dirac case, $2n - 1$ phases can be removed by a proper re-phasing of the left-handed fields, leaving $(n-1)(n-2)/2$ physical phases. Therefore, $\mathcal{CP}$ violation is only possible in the case of $n \geq 3$ generations. In the Majorana case there is less freedom to re-phase the fields, since the phases of the neutrino fields cannot be absorbed in the Majorana mass terms. Only n phases can be removed, leaving $n(n-1)/2$ physical phases. Out of these $(n-1)(n-2)/2$ are the usual Dirac phases, while $n-1$ are specific to the Majorana case and are called Majorana phases. The latter do not lead to any observable effects in neutrino oscillations and are not discussed further in this review.

In the simple case of two families, this matrix reduces to the rotation matrix:

$$\begin{pmatrix} \nu_e \\ \nu_\mu \end{pmatrix} = \begin{pmatrix} \cos\theta & \sin\theta \\ -\sin\theta & \cos\theta \end{pmatrix} \begin{pmatrix} \nu_1 \\ \nu_2 \end{pmatrix} \tag{1}$$

where the angle θ is called the neutrino mixing angle, since it mixes the mass eigenstates ν_1 with mass m_1 and ν_2 with mass m_2.

If one assumes that a given source is producing a neutrino flux of given flavor $|\nu_\alpha\rangle$ at $t = x = 0$, the neutrino state at a later time t is then $|\nu(t)\rangle = U^*_{\alpha j}e^{-iE_j t}|\nu_j\rangle$, and evolves as an admixture of the mass eigenstates. The probability amplitude of finding the neutrino at the time t in a flavour state ν_β is

$$A(\nu_\alpha \to \nu_\beta; t) = U_{bj}e^{-iE_j t}U^*_{aj} . \tag{2}$$

The neutrino oscillation probability, i.e. the transformation probability of a flavour eigenstate neutrino $|\nu_\alpha\rangle$ into another one $|\nu_\beta\rangle$ is then

$$P(\nu_\alpha \to \nu_\beta; t) = |A(\nu_\alpha \to \nu_\beta; t)| = |U_{bj}e^{-iE_j t}U^*_{aj}|^2 \tag{3}$$

Therefore the probability for detecting a state of a different flavor ν_β, at a given distance L from the source, is given, for relativistic particles, by:

$$P(\nu_\alpha \to \nu_\beta) \approx \sin^2 2\theta \, \sin^2(1.27\Delta m^2 \frac{L}{E}) \tag{4}$$

where L is in m (km) and E in MeV (GeV). The mixing angle θ Eqs.(1) and (4) determines the oscillation amplitude, whereas the difference of the square of the masses $\Delta m^2 = m_1^2 - m_2^2$, gives the oscillation frequency (Figure 1). The neutrino sources available (the sun, the atmosphere, reactors and accelerators) have different typical neutrino average energies, and distances between the source and the detector, and allow to probe various oscillation frequencies. Oscillation searches are called appearance experiments, if the appearance of a new flavour is looked for, or disappearance experiments, if a reduction in the neutrino flux from the source is searched for.

Neutrino propagation through matter can modify oscillations significantly. This is known as the Mikheyev-Smirnov-Wolfenstein (MSW) effect (Mikheev and Smirnov 1986, Wolfenstein 1978). Indeed, neutrinos of all flavors couple to electrons, protons
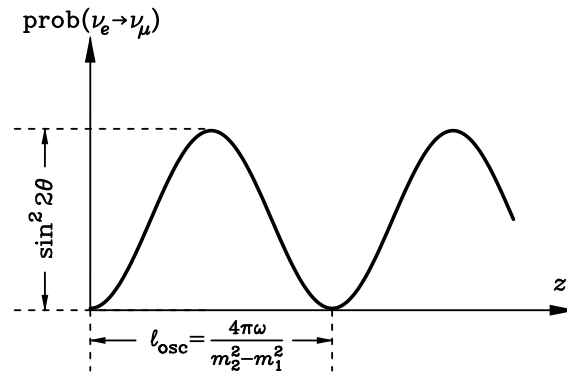
Figure 1. Schematic drawing of the ν_e to ν_μ appearance oscillation probability in the case of two families Eq.(4). The oscillation amplitude and frequency depend on two neutrino parameters: θ and $\Delta m^2 = m_2^2 - m_1^2$, where m_1 and m_1 are the masses of the mass eigenstates ν_1 and ν_2 respectively.

and neutrons in matter through neutral currents. In the case of ν_e scattering through charged-currents is also effective. This scattering induces a matter-induced potential acting on the electron neutrinos, which depends on the electron density n_e:

$$V_e^{CC} = \sqrt{2} G_F n_e. \tag{5}$$

The neutral current contributions from electrons and protons cancel, if the medium is electrically neutral, whereas the scattering on neutrons induces equal potentials on all neutrinos. Staying in the two-flavor formalism, the time evolution of the flavor eigenstates is as follows§:

$$i\frac{d}{dt}\begin{pmatrix} \nu_e \\ \nu_\mu \end{pmatrix} = \begin{pmatrix} -\frac{\Delta m^2}{4E}\cos 2\theta + \sqrt{2}G_F n_e & \frac{\Delta m^2}{4E}\sin 2\theta \\ \frac{\Delta m^2}{4E}\sin 2\theta & \frac{\Delta m^2}{4E}\cos 2\theta \end{pmatrix}\begin{pmatrix} \nu_e \\ \nu_\mu \end{pmatrix}. \tag{6}$$

Note that in the three-flavor formalism, the matter-induced potential modifies both ν_e versus ν_μ and ν_μ to ν_τ oscillations, since these are coupled. Matter effects can enhance neutrino oscillations when the MSW resonance condition is met:

$$\frac{\Delta m^2}{2E}\cos 2\theta = \sqrt{2}G_F n_e \ . \tag{7}$$

This means, that independently on the value of the vacuum mixing angle θ, mixing in matter is maximal if the MSW condition Eq.(7) is satisfied.

In the case of three families, the neutrino flavour and mass eigenstates are related through

$$\begin{pmatrix} \nu_e \\ \nu_\mu \\ \nu_\tau \end{pmatrix} = \begin{pmatrix} U_{e1} & U_{e2} & U_{e3} \\ U_{\mu1} & U_{\mu2} & U_{\mu3} \\ U_{\tau1} & U_{\tau2} & U_{\tau3} \end{pmatrix}\begin{pmatrix} \nu_1 \\ \nu_2 \\ \nu_3 \end{pmatrix} \tag{8}$$

§ Terms which contribute equally to the diagonal give equal phases and do not influence neutrino oscillations.
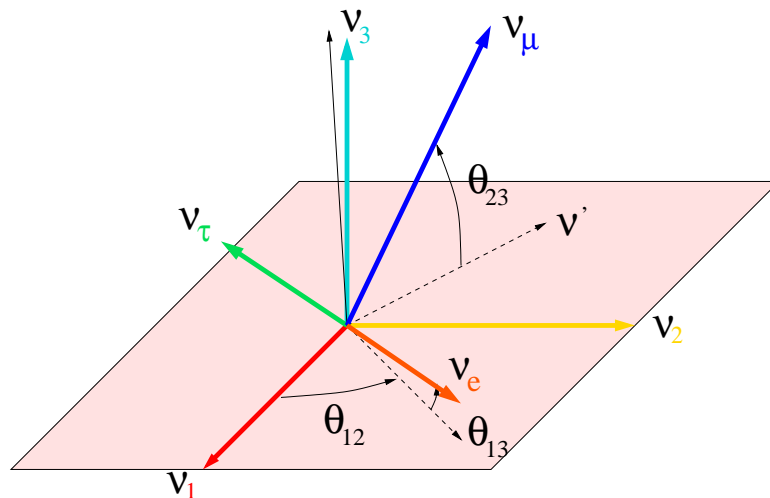
Figure 2. Representation of the 3-d "rotation" relating the neutrino flavour and mass basis Eqs.(8-9).

This matrix is called the Maki-Nakagawa-Sakata-Pontecorvo (MNSP) matrix, the analogue of the Cabibbo-Kobayashi-Maskawa (CKM) matrix, and is usually parametrized as:

$$U = \begin{pmatrix} c_{12}c_{13} & s_{12}c_{13} & s_{13}e^{-i\delta} \\ -s_{12}c_{23} - c_{12}s_{23}s_{13}e^{i\delta} & c_{12}c_{23} - s_{12}s_{23}s_{13}e^{i\delta} & s_{23}c_{13} \\ s_{12}s_{23} - c_{12}c_{23}s_{13}e^{i\delta} & -c_{12}s_{23} - s_{12}c_{23}s_{13}e^{i\delta} & c_{23}c_{13} \end{pmatrix} \tag{9}$$

where $c_{ij} = \cos\theta_{ij}$ and $c_{ij} = \sin\theta_{ij}$, θ_{ij} are the rotation angles (Figure 2) and δ is a $\mathcal{CP}$ Dirac violating phase. If neutrinos are Majorana particles, the matrix U is multiplied by an additional matrix having only non-zero diagonal terms, i.e. $diag(1, e^{i\alpha_1}, e^{i\alpha_2})$, including two extra $\mathcal{CP}$ violating phases. As far as the oscillation frequencies are concerned, since $\sum_i \Delta m_i^2 = 0$, only two frequencies are independent. Note that the oscillation phenomenon gives information on the Δm_i^2 only, while the neutrino mass scale needs to be obtained from other measurements, in particular from the endpoint spectrum of nuclear beta-decay - like the tritium based experiment KATRIN (Angrik *et al* 2004) - or from the possible observation of the neutrinoless double-beta decay in nuclei, where the latter is also sensitive to the neutrino nature and to the Majorana $\mathcal{CP}$ violating phases (see e.g. Elliott and Engel 2004).

In the last years much progress has been obtained in our knowledge of neutrino properties (for a detailed description see e.g. Bilenky *et al* 2003). Two Δm^2 and mixing angles are now known, i.e. $\Delta m_{12}^2 = 7.9 \ 10^{-5} \ \text{eV}^2$, $\sin^2\theta_{12} = 0.3$, and $\Delta m_{23}^2 = 2.4 \ 10^{-3} \ \text{eV}^2$, $\sin^2\theta_{23} = 0.5$, often referred to as the solar and the atmospheric oscillation parameters respectively, extracted from the SNO (Ahmad *et al* 2001) and KAMLAND (Eguchi *et al* 2003) experiments on one hand, and from the Super-Kamiokande (Fukuda *et al* 1998) and K2K (Ahn *et al* 2003) experiments on the other hand. The sign of the solar oscillation parameter Δm_{12}^2 is known, while the atmospheric one Δm_{23}^2 remains unknown. This introduces degeneracies in the determination of the
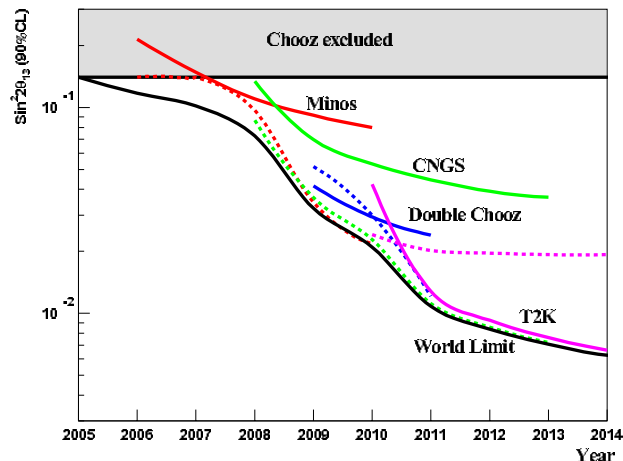
Figure 3. Sensitivity on $\sin^2 2\theta_{13}$ as a function of time. For each experiment, its sensitivity is shown (solid line), as well as the world sensitivity without the experiment (dashed line). The overall world as a function of time is also shown (Guglielmi *et al* 2005).

other unknown parameters (Section V). Note that the LSND collaboration has found a positive oscillation signal at $\Delta m^2 = 1 \, \text{eV}^2$ as well (Athanassopoulos *et al* 1998 and 1996). The running miniBOONE and the future BOONE experiments will confirm/refute these observations. Waiting for these results, in this review, we will not consider the third oscillation frequency and will stay within the three flavour formalism.

The precise value of the θ_{13} angle is not yet known, the present upper limit $\sin^2 2(\theta_{13}) < 0.1$ is extracted from a reactor experiment called CHOOZ (Apollonio *et al* 1999). Future experiments will improve the present sensitivities on $\sin^2 2\theta_{13}$ and search first in the $10^{-1} - 10^{-2}$ range (Figure 3). The $10^{-3} - 10^{-4}$ range will only be reached with beta-beams while values smaller than 10^{-4} can be explored with a neutrino factory. It is important to remind that the knowledge of θ_{13} is crucial for $\mathcal{CP}$ violation searches, since if by any chance nature has decided that θ_{13} is strictly zero, there cannot be any $\mathcal{CP}$ violation through the Dirac δ phase.

1.2. $\mathcal{CP}, \mathcal{T}, \mathcal{CPT}$ violation searches

The study of the weak interaction and of neutrino properties has brought some of the building blocks of the Standard Model. Since 1964, we know that $\mathcal{CP}$ is one of the symmetries broken by the weak interaction, as first observed in K mesons (Christenson *et al* 1964), and recently in B mesons. The $\mathcal{CPT}$ theorem ensures that under given conditions (Lorentz invariance, locality of the interactions) a modern quantum field theory description of particles and their interactions preserves the $\mathcal{CPT}$ symmetry. This is the case for renormalizable abelian theories. However some variants of string theories predict a breaking of Lorentz invariance and therefore of the $\mathcal{CPT}$ symmetry. Note that an obvious consequence of $\mathcal{CP}$ violation is the violation of the $\mathcal{T}$ symmetry.

Neutrinos can be used to study these symmetries and their breaking through the comparison of neutrino oscillations. If $\mathcal{CP}$ is conserved, the oscillation probability between particles and between the corresponding antiparticles coincide:

$$\mathcal{CP} \quad : \qquad P(\nu_a \rightarrow \nu_b; t) = P(\bar{\nu}_a \rightarrow \bar{\nu}_b; t). \tag{10}$$

The action of the particle-antiparticle conjugation on the lepton mixing matrix U Eq.(9) amounts to the change $U \rightarrow U^*$, meaning that $\mathcal{CP}$ is only conserved if the mixing matrix U is real or can be made real by re-phasing of the lepton fields. The search for the possible existence of $\mathcal{CP}$ violation in the lepton sector and of a non-zero the Dirac phase δ Eq.(9) consists in searching for possible differences between neutrino versus anti-neutrino oscillations.

Time reversal interchanges the initial and the final states, so if $\mathcal{T}$ is conserved one has:

$$\mathcal{T} \quad : \qquad P(\nu_a \rightarrow \nu_b; t) = P(\nu_b \rightarrow \nu_a; t). \tag{11}$$

Finally, the oscillation probabilities are invariant under the combined action of $\mathcal{CP}$ and $\mathcal{T}$, if the following equality holds:

$$\mathcal{CPT} \quad : \qquad P(\nu_a \rightarrow \nu_b; t) = P(\bar{\nu}_b \rightarrow \bar{\nu}_a; t). \tag{12}$$

The study of these symmetries requires in particular appearance oscillation experiments, since disappearance experiments like $P(\nu_e \rightarrow \nu_e)$ are time-reversal invariant, and clearly insensitive to $\mathcal{CP}$ breaking effects. For example, by using Eqs.(3) and (8-9), the $\nu_\mu \rightarrow \nu_e$ appearance probability can be rewritten as :

$$P(\nu_\mu \rightarrow \nu_e) = 4c_{13}^2 s_{13}^2 s_{23}^2 \sin^2 \frac{\Delta m_{13}^2 L}{4E_\nu} \times \left[1 + \frac{2a}{\Delta m_{13}^2}(1 - 2s_{13}^2) \right] \tag{13}$$

$$+ 8c_{13}^2 s_{12} s_{13} s_{23}(c_{12}c_{23}\cos\delta - s_{12}s_{13}s_{23}) \cos \frac{\Delta m_{23}^2 L}{4E_\nu} \sin \frac{\Delta m_{13}^2 L}{4E_\nu} \sin \frac{\Delta m_{12}^2 L}{4E_\nu}$$

$$- 8c_{13}^2 c_{12} c_{23} s_{12} s_{13} s_{23}\sin\delta \sin \frac{\Delta m_{23}^2 L}{4E_\nu} \sin \frac{\Delta m_{13}^2 L}{4E_\nu} \sin \frac{\Delta m_{12}^2 L}{4E_\nu}$$

$$+ 4s_{12}^2 c_{13}^2 (c_{13}^2 c_{23}^2 + s_{12}^2 s_{23}^2 s_{13}^2 - 2c_{12}c_{23}s_{12}s_{23}s_{13} \cos\delta) \sin \frac{\Delta m_{12}^2 L}{4E_\nu}$$

$$- 8c_{12}^2 s_{13}^2 s_{23}^2 \cos \frac{\Delta m_{23}^2 L}{4E_\nu} \sin \frac{\Delta m_{13}^2 L}{4E_\nu} \frac{aL}{4E_\nu}(1 - 2s_{13}^2).$$

The first line contains terms driven by θ_{13}, the second and third lines contain $\mathcal{CP}$ even and odd terms respectively, while the forth line is driven by the solar parameters (Figure 4). Matter effects developed at the first order are included in the last line, where $a[\text{eV}^2] = \pm 2\sqrt{2}G_F n_e E_\nu = 7.610^{-5}\rho[\text{g/cm}^3]E_\nu[\text{GeV}]$. The $\mathcal{CP}$ odd term as well as matter effects change sign by replacing neutrinos with anti-neutrinos. The occurrence of matter effects, at baselines of about $O(1000)$ km (Figure 5), allows to extract information on the mass hierarchy, since their sign depends on the sign of Δm_{23}^2. These effects can be distinguished from the true $\mathcal{CP}$ violating ones, because they have a different energy dependence.
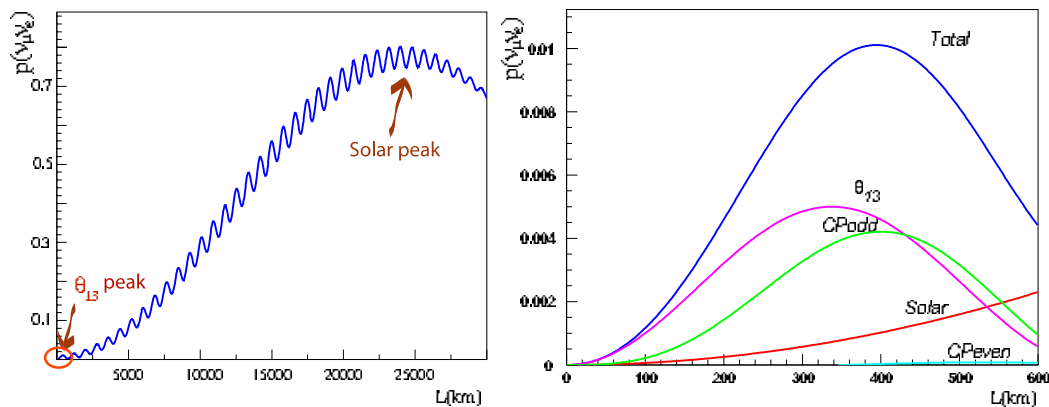
Figure 4. Drawing of the $P(\nu_\mu \to \nu_e)$ oscillations as a function of the distance, assuming a monochromatic beam of 1 GeV neutrinos, and matching the solar oscillation frequency for $\delta = 0$ (left figure) and the atmospheric oscillation frequency for $\delta = -\pi/2$ (right figure). In the latter case, the different terms contributing to the oscillation probability Eq.(14) are shown (Guglielmi *et al* 2005).

Clearly, the knowledge of the Dirac δ phase depends on the knowledge of all other oscillation parameters at the time an experiment searching for $\mathcal{CP}$ violation takes place. As mentioned above, a particularly important piece of information is the value of the angle θ_{13}. Note that if $\theta_{13} \neq 0$, it might be difficult from one single experiment to unambiguously extract information about θ_{13} and δ because of the correlations and the degeneracies (Section V). Anyway, pure, intense and collimated neutrino beams are needed to determine very small θ_{13} values and a non-zero phase, such as those produced with beta-beams.

2. The original beta-beam scenario

2.1. The beta-beam concept and neutrino fluxes

When a nucleus undergoes a beta-decay, it emits either an electron neutrino, or an electron anti-neutrino. In the rest frame of the nucleus, such neutrinos are emitted isotropically. However, if the ions are accelerated, the momentum parallel to the ion beam gets boosted, while the perpendicular one keeps unchanged. As a consequence, the neutrino beam gets collimated with the emittance of the neutrino flux inversely proportional to the Lorentz gamma factor. A neutrino beam produced with this procedure is what we call, a "beta-beam" (Zucchelli 2002). The neutrino flux is well known, since the ion intensity can be precisely determined and the flux is pure in flavour. Its expression can be determined analytically as follows (Serreau and Volpe 2004).

The decay rate of a nucleus in the rest (cm) frame can be written as:

$$\frac{dW}{dt}\bigg|_{cm} = \Phi_{cm}(E_\nu)\, dE_\nu\, \frac{d^2\Omega}{4\pi}\,, \tag{14}$$

where E_ν and Ω denote respectively the energy and the solid angle of the emitted
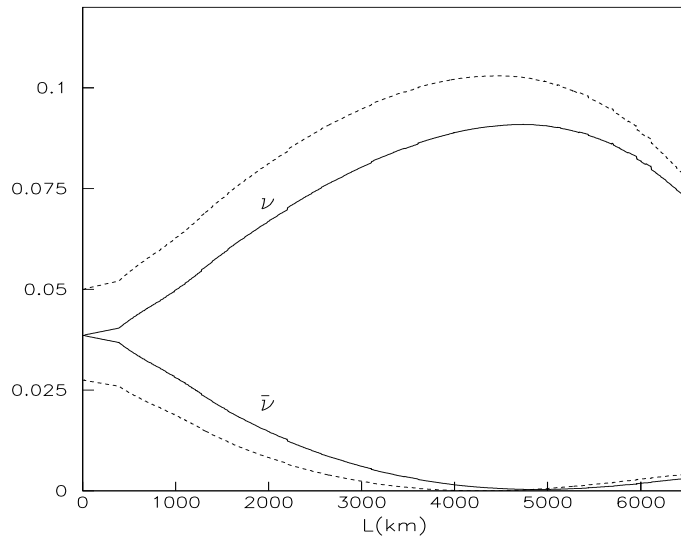
Figure 5. Comparison of the $\nu_e \rightarrow \nu_\mu$ and the $\bar{\nu}_e \rightarrow \bar{\nu}_\mu$ appearance oscillation probability, as a function of the baseline distance L between the source and the detector, evaluated at the first atmospheric oscillation maximum $E/L = |\Delta m_{23}^2|/2\pi$. From about $L = O(1000)$ km, matter effects becomes significant and can be exploited to extract the sign of Δm_{23}^2. The solid and dashed curves show the true $\mathcal{CP}$ violation effects for $\delta = 0$ and $90°$.

(anti)neutrino, and where the neutrino flux $\Phi_{cm}(E_\nu)$ is given by the well-known formula:

$$\Phi_{cm}(E_\nu) = b\, E_\nu^2\, E_e\, \sqrt{E_e^2 - m_e^2}\, F(\pm Z, E_e)\, \Theta(E_e - m_e)\,. \tag{15}$$

where the constant $b = \ln 2/m_e^5 ft_{1/2}$, with m_e the electron mass and $ft_{1/2}$ the ft-value. The quantities appearing in the above expression are the energy $E_e = Q_\beta - E_\nu$ of the emitted lepton (electron or positron), Q_β is the Q_β–value of the decay. The Fermi function $F(\pm Z, E_e)$ accounts for the Coulomb modification of the spectrum.

In the laboratory frame, where the boosted nucleus has a velocity $v = \beta c$, the decay rate reads:

$$\left.\frac{dW}{dt}\right|_{lab} = \frac{1}{\gamma}\, \Phi_{lab}(E_\nu, \theta)\, dE_\nu\, \frac{d^2\Omega}{4\pi}\,, \tag{16}$$

where $\gamma = 1/\sqrt{1 - \beta^2}$ is the time dilation factor and where E_ν and $\Omega \equiv (\theta, \varphi)$ now denote the energy and solid angle of the emitted (anti)neutrino in the laboratory (*lab*) frame, θ being the angle of emission with respect to the beam axis. The boosted flux $\Phi_{lab}(E_\nu, \theta)$ is given by:

$$\Phi_{lab}(E_\nu, \theta) = \frac{\Phi_{cm}(E_\nu \gamma[1 - \beta\cos\theta])}{\gamma[1 - \beta\cos\theta]}\,. \tag{17}$$

The ions are stored in a storage ring of total length S with straight sections of length D. In the stationary regime the mean number of ions in the storage ring is $\gamma\tau g$, where $\tau = t_{1/2}/\ln 2$ is the lifetime of the parent nuclei and g is the number of injected ions

per unit time. The total number of neutrinos emitted per unit time from a portion $d\ell$ of the decay ring is therefore

$$\frac{dN_\nu}{dt} = \gamma\tau\, g \times \left.\frac{dW}{dt}\right|_{lab} \times \frac{d\ell}{S}\,. \tag{18}$$

Let us consider, for example, a cylindrical detector of radius R and depth h, aligned with one of the the storage ring straight sections, and placed at a distance d from the latter. After integration over the useful decay path and over the volume of the detector, the total number of events per unit time is:

$$\frac{dN_{ev}}{dt} = g\tau nh \times \int_0^\infty dE_\nu\, \Phi_{tot}(E_\nu)\,\sigma(E_\nu)\,, \tag{19}$$

where n is the number of target nuclei per unit volume, $\sigma(E_\nu)$ is the relevant interaction cross section with the target, and the total neutrino flux is

$$\Phi_{tot}(E_\nu) = \int_0^D \frac{d\ell}{S} \int_0^h \frac{dz}{h} \int_0^{\bar\theta(\ell,z)} \frac{\sin\theta d\theta}{2}\, \Phi_{lab}(E_\nu,\theta)\,, \tag{20}$$

with

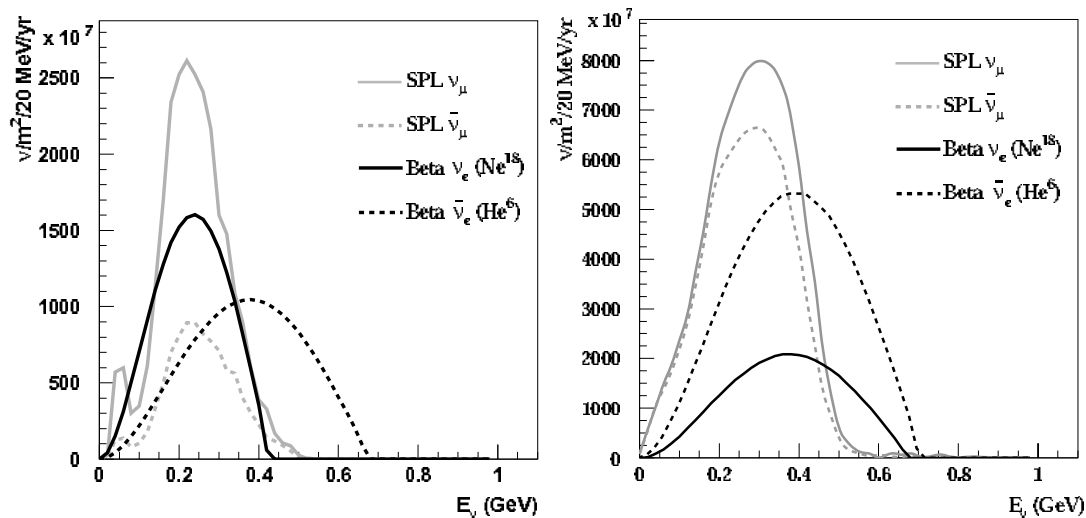$$\tan\bar\theta(\ell,z) = \frac{R}{d+\ell+z}\,. \tag{21}$$

Figure 6. Comparison of neutrino fluxes from a super-beam (SPL) and a beta-beam. The neutrino beams are produced at CERN and sent to the Fréjus Underground Laboratory, 130 km from CERN. Two options for the beta-beam are shown here. Left: The ions circulate together in the storage ring, with $\gamma = 60$ (100) for ^{6}He (^{18}Ne) (Mezzetto 2005). Right: The ions circulate at the same $\gamma = 100$, independently, in the storage ring. Note that the average neutrino energies are related to the ion boost through $E_\nu \approx 2\gamma Q_\beta$ (Guglielmi *et al* 2005).

Figures 6 and 7 show examples of the neutrino fluxes from beta-beams where the ions are boosted at γ of several hundreds or from low energy beta-beams with $\gamma = 7-14$, respectively.
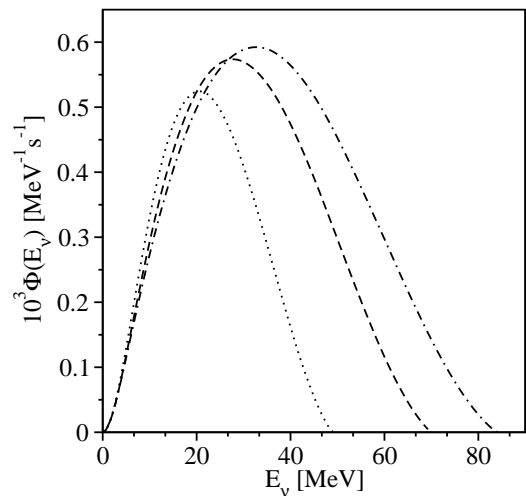
Figure 7. Anti-neutrino fluxes from low energy beta-beams. The curves correspond to $\gamma = 7$ (dotted line), $\gamma = 10$ (broken line) and $\gamma = 12$ (dash-dotted line) for the boosted helium-6 ions. Similar curves are obtained for neutrinos from neon-18 ions. The detector is located at 10 m from a small devoted storage ring (see Section III) (Balantekin *et al* 2006a).

2.2. The baseline

The original conceptual design for a beta-beam beam facility includes three main steps (Zucchelli 2002, Autin *et al* 2002, Bouchez *et al* 2003, Benedikt *et al* 2004, Lindroos and Volpe 2004, Benedikt 2005). In the first stage protons delivered by a Superconducting Proton Linac (SPL) impinge on a target to produce radioactive species of interest, using an ISOL target. Such an intense proton driver (at present under study) would deliver 2mA of 2.2 GeV (kinetic energy) protons, while the ISOL target would need 100 μA, that is 5 % of the proton intensity only. After ionization and bunching, the ions are accelerated to low energy, i.e. 300 MeV/A. This part of the facility is very close to the conceptual design of the EURISOL project (see EURISOL), aiming to the production and acceleration of very intense radioactive ion beams through the ISOL technique. In the second stage energies of about 100 GeV/A are attained using e.g. CERN accelerator infrastructures, like the PS and SPS. Finally the ions are stacked longitudinally in a new decay ring. Each of these steps require specific feasibility studies, in particular the bunching at low energy, space-charge limitations in the PS and SPS (keeping CERN in mind as a possible site), decay losses in the accelerator chain and, at high energy, the stacking process in the decay ring. Both the decay ring, the proton source and the low energy accelerators do not exist at CERN today. Nevertheless, the use of existing accelerator infrastructure represents an important saving. The beta-beam complex is shown schematically in Figure 8.

The choice of the isotopes is based on several criteria. The half-life should be such as to minimize the decay losses in the accelerator chain. Another constraint comes from the required collimation and energy of the neutrinos at the detector, which depends on

the energy of the decaying ions through $E_\nu \approx 2\gamma Q_\beta$. These (and other) considerations point at present at two isotopes of particular interest, namely ^{6}He and ^{18}Ne as antineutrino and neutrino emitters respectively. Their lifetimes are 0.8 s and 1.6 s, while their Q_β-values are of about 4 MeV. Both these ions can be produced in large quantities by the so-called ISOL method. These two noble gases have the advantage that they can easily diffuse from the target. For helium, it consists either of a water cooled tungsten core or of a liquid lead core which works as a proton to neutron converter surrounded by a beryllium oxide, aiming for 10^{15} fissions per second. This yields a quasi-continuous beam, so the ions have to be bunched prior to further acceleration. Efficient bunching and full stripping of a high-intensity beam can be achieved using a high frequency ECR source (Sortais 2003). While such system does not exist today, theoretical calculations show that one can be constructed.

16 bunches (consisting for example of 2.5 10^{12} ions each for helium) are first accumulated in the PS, reduced to 8 bunches during the acceleration to intermediate energies, injected in the SPS and then in the storage ring in batches of four 10 ns bunches. This time structure is required to efficiently reduce the atmospheric background. Note that the SPS can accelerate ^{6}He and ^{18}Ne ions at a maximum γ value of 150 and of 250 respectively (Lindroos 2005). Due to the relativistic time dilatation, the ion lifetimes reach several minutes, so that stacking the ions in the decay ring is mandatory to get enough decays and hence high neutrino fluxes. The ring has the shape of an hippodrome, with a total length of 6880 m and straight sections of 2500 m each (36 %). The average number of ions in the storage ring between two stacking cycles is given by $N_{average} = N_{bunch}\gamma\tau/T$ where N_{bunch} is the number of particles with mean-life τ having Lorentz boost γ, injected into the ring every T seconds.

The ion injection and merging with existing high density bunches in the decay ring represent an important challenge and require a new scheme. Stacking means a regular top-up of the stored beam before the existing particles cease to be useful. Many stacking methods involve some form of a beam cooling to increase phase space density and make room for more particles within a given transverse and longitudinal acceptance. For light ions at high energy, the classical methods of electron and stochastic cooling are excluded. Instead, a new scheme has been proposed combining bunch rotation and asymmetric bunch pair merging. The new bunches are off momentum and are injected in a high dispersion region on a matched dispersion trajectory. Subsequently, each injected bunch rotates a quarter turn in longitudinal phase space until the initial conditions for bunch pair merging are met. In the final step, each small fresh bunch is moved into the core of a large stored one and then phase space mixing occurs. The fact that only the central part of the existing bunch is combined with an incoming dense one results in a net increase in the core intensity of the resultant stored beam. The surrounding older ions are pushed out toward the bucket separatrix, where eventually the oldest are lost. This new method, called asymmetric bunch pair merging, has recently been demonstrated at the CERN PS.

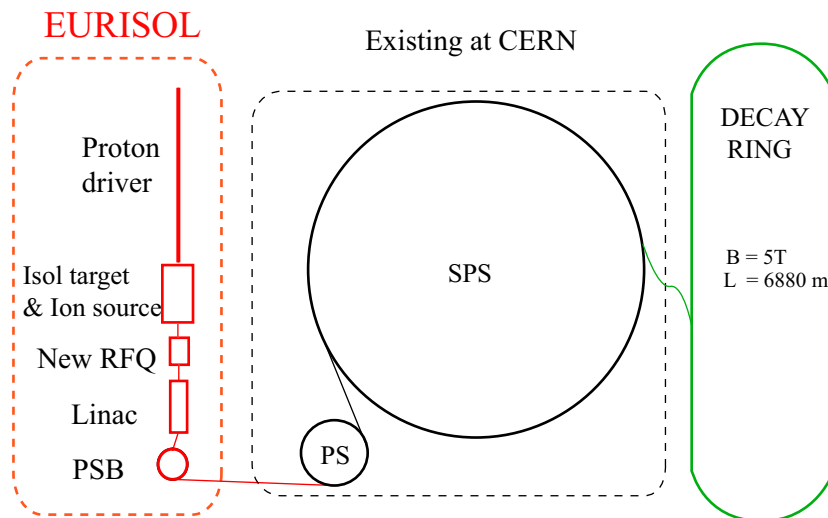A principal difference between the acceleration to high energies of stable and

Figure 8. Schematic drawing of a beta-beam facility complex at CERN. The production, collection and acceleration part shown on the left is very close to the EURISOL project (see EURISOL), at present under study, which aims at producing very intense radioactive ion beams. The ions are then injected in the Proton-Synchrotron (PS) and Super Proton-Synchrotron (SPS) accelerator infrastructures (central part) already existing at CERN, to achieve about a hundred GeV per nucleon ($\gamma = 100$). Finally the ions are stored to decay in an hippodrome-like storage ring (right part), that needs to be built. One of the long straight sections points to a far detector (Zucchelli 2002, Autin *et al* 2003).

radioactive ions is the additional losses due to the radioactive decays. The predicted intensities for ^{6}He and ^{18}Ne are shown in Table 1. The conventional losses through the accelerator chain are expected to be less than 50 % (based on operational experience at CERN). The isotopes proposed for the beta-beam conceptual design have been chosen such that no long-lived activity is left to contaminate the low energy machines. A first simulation of losses in the decay ring yields a dose rate in the arcs of 2.5 mSv/h after 30 days of operation and one day of cooldown. Furthermore, the induced radioactivity in the ground water will have no impact on public safety. It has also been confirmed that the total loss in the accelerator chain will be beyond the nominal 1 W/m that permits hands-on maintenance (except for the PS).

2.3. Sensitivity to $\mathcal{CP}$ violation

The major goal of the beta-beam facility proposed by (Zucchelli 2002) is to measure $\mathcal{CP}$ violation in the lepton sector. This requires a comparison of neutrino versus anti-neutrino oscillations in an appearance experiment Eq.(10) (note that disappearance experiments like $\nu_e \rightarrow \nu_e$ are not sensitive to the $\mathcal{CP}$ violating phase δ). Since beta-beams produce pure electron neutrino (or anti-neutrino) beams, such experiment should search for differences in $\nu_e \rightarrow \nu_\mu$ versus $\bar{\nu}_e \rightarrow \bar{\nu}_\mu$ oscillations Eq.(14). The scenario considered is to produce the neutrino beams at CERN (Figure 8) and fire them to a

Table 1. Intensities for the ^{6}He and ^{18}Ne ion beams along the acceleration chain. Only beta-decay losses are taken into account. The number of ions in the decay ring, including conventional losses, is $0.5N_{tot}$ (Autin *et al* 2002, Lindroos 2003, Benedikt *et al* 2004, Benedikt 2005).

Machine	^{6}He ions extracted	^{18}Ne ions extracted	Batches
Source	$2\ 10^{13}$	$8\ 10^{11}$ ions/s	dc
Rapid Cycling Synchrotron	$1.00\ 10^{12}$	$4.09\ 10^{10}$	16
PS	$1.01\ 10^{13}$	$5.19\ 10^{11}$	1
SPS	$0.95\ 10^{13}$	$4.90\ 10^{11}$	∞
Decay Ring (N_{tot})	$2.02\ 10^{14}$	$9.11\ 10^{12}$	-

water Čerenkov detector of 440 kton fiducial volume – like MEMPHYS (Mosca 2005a, Campagne *et al* 2006), UNO (Jung 2000), or HYPER-K (Itow *et al* 2001) – located at the (upgraded) Fréjus Underground Laboratory, 130 km from CERN. If Lorentz ion boosts around 60-100 are chosen (Fig.6), this distance magically fits the $\nu_e \to \nu_\mu$ first oscillation maximum at the atmospheric scale (Fig.4). The detector is of the same kind of Super-Kamiokande (Fukuda *et al* 1998), but has a fiducial mass 20 times larger, requiring a cavern of about 1 million cubic meters. The ion intensity considered is $2.9\ 10^{18}$ ^{6}He and $1.1\ 10^{18}$ ^{18}Ne per year (Autin *et al* 2003).

The physics potential of the original baseline scenario is being actively investigated (Mezzetto 2003, Bouchez *et al* 2003, Mezzetto 2005a, Mezzetto 2005b, Campagne *et al* 2006) and is discussed in (Guglielmi *et al* 2005, Mosca 2005b). The signal corresponds to the muons produced by ν_μ charged-current events in water, mainly via quasi-elastic interactions at these energies. Such events are selected by requiring a single-ring event, with the same identification algorithms used by the Super-Kamiokande experiment (Fukuda *et al* 1998), and by the detection of the electron from the muon decay. At such energies the energy resolution is very poor due to the Fermi motion and other nuclear effects. For these reasons, a $\mathcal{CP}$ violation search with $\gamma = 60 - 100$ is based on a counting experiment only. Energy cuts can be exploited when going to higher γ, as first suggested in (Burguet-Castell 2004) (see Section IV) e.g. to resolve some of the degeneracies and get information on the neutrino hierarchy.

The beta-beam has no intrinsic backgrounds, contrary to conventional sources. However, inefficiencies in particle identification, such as single-pion production in neutral-current ν_e ($\bar{\nu}_e$) interactions, electrons (positrons) misidentified as muons, as well as external sources, like atmospheric neutrino interactions, can produce backgrounds. The background coming from single pion production has a threshold at about 450 MeV, therefore giving no contribution for $\gamma < 55$. Standard algorithms for particle identification in water Čerenkov detectors are quite efficient in suppressing the fake signal coming from electrons (positrons) misidentified as muons, especially if the signal for the muon decaying into electrons is also required. Concerning the atmospheric

Table 2. Number of events expected after 10 years, for a beta-beam produced at CERN (Figure 8) and sent to a 440 kton water Čerenkov detector located at an (upgraded) Fréjus Underground Laboratory, at 130 km distance. The results correspond to $\bar{\nu}_e$ (left) and ν_e (right). The different γ values are chosen to make the ions circulate together in the ring (Mezzetto 2005a).

	^{6}He ($\gamma = 60$)	^{18}Ne ($\gamma = 100$)
CC events (no oscillation)	19710	144784
Oscillated ($\sin^2 2\theta_{13} = 0.12$, $\delta = 0$)	612	5130
Oscillated ($\delta = 90°$, $\theta_{13} = 3°$)	44	529
Beam background	0	0
Detector backgrounds	1	397

neutrino interactions, estimated to be of about 50/kton/yr, this important background is reduced to 1 event/440 kton/yr by requiring a time bunch length for the ions of 10 ns.

The choice of the ion acceleration is a compromise between having the γ factor as high as possible, to profit of larger cross sections and better focusing of the beam on one hand, and keeping it as low as possible to minimize the single pion background and better match the $\mathcal{CP}$ odd terms Eq.(14) on the other hand. If one requires the ions to circulate together in the decay ring (Figure 8), this constraints the ratio of the ion boosts to be $\gamma(^6\text{He})/\gamma(^{18}\text{Ne})=3/5$. In this case the optimal boosts turn out to be $\gamma(^6\text{He})=60$ and $\gamma(^{18}\text{Ne})=100$, giving 0.24 GeV and 0.36 GeV as $\bar{\nu}_e$ and ν_e average energies respectively (Figure 6 left). This choice is assumed in (Bouchez *et al* 2003, Mezzetto 2005a).

Table 2 shows the expected events with and without oscillations. One can see that the beam related background is zero, while some background events are expected especially for the case of neon-18, due to the single-pion misidentified events. The expected sensitivity on θ_{13} is shown in Figure 9 after 5 years run, in comparison with planned or proposed experiments. Note that the value of this angle can be explored both with $\bar{\nu}_e$ and ν_e disappearance and with $\bar{\nu}_\mu$ and ν_μ appearance experiments. Clearly, a beta-beam alone as well as a combination of a super-beam and a beta-beam sent to the same detector are powerful and allow to reach sensitivities on $\sin^2 2\theta_{13}$ in the range of $10^{-3} - 10^{-4}$, improving the present CHOOZ upper limit (Apollonio *et al* 1999) by a factor of about 200.

The sensitivity in the (θ_{13}, δ) plane is shown in Figure 10, having fixed the other oscillation parameters to the values $\sin^2 2\theta_{23} = 1$, $\Delta m_{23}^2 = 2.5\ 10^{-3}\text{eV}^2$, $\text{sign}(\Delta m_{23}^2)=+1$, $\sin^2 2\theta_{12} = 0.8$, $\Delta m_{12}^2 = 7.1\ 10^{-5}\text{eV}^2$. The assumed corresponding errors are of 5 % and of 1% on Δm_{23}^2 and on $\sin^2 2\theta_{23}$ respectively, as expected from the T2K experiment (Itow *et al* 2001), while 10 % error is taken for the solar oscillation parameters. The curves are determined by fitting the number of muon-like events in the $\bar{\nu}_\mu$ and ν_μ oscillation experiments simultaneously (Table 2). Correlations between
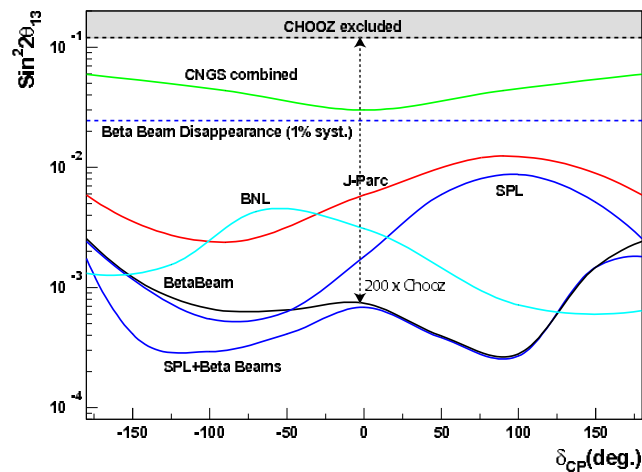
Figure 9. Sensitivity on θ_{13} (90 % C.L.) as a function of δ for a beta-beam, a super-beam (SPL), and their combination. The present CHOOZ limit (Apollonio *et al* 1999) is shown, as well as the sensitivities of CNGS and JPARC (Migliozzi and Terranova 2003) and BNL (Diwan *et al* 2003). The appearance results are calculated considering 5 years measuring time (Mezzetto 2005a).
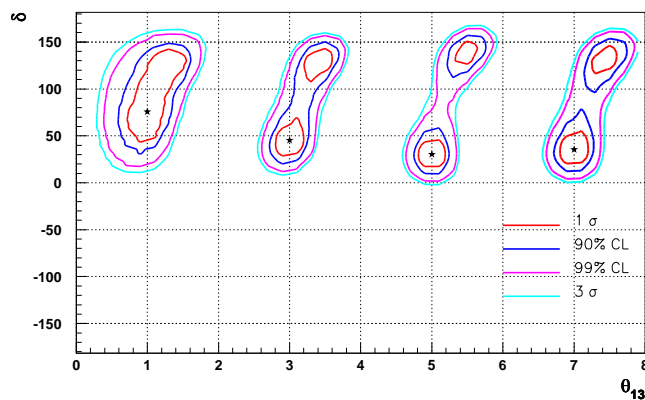

Figure 10. Fits to θ_{13} and δ after ten years measurement time, computed with the events shown in Table 2. The stars indicate the parameters' values, while the different curves show the various confidence levels (Mezzetto 2005a).

θ_{13} and δ are fully accounted for and have a negligible effect (Figure 10, see section V for a discussion on the intrinsic degeneracy). The ambiguity on the sign of Δm_{23}^2 is translated in a direct ambiguity on the sign of δ, since matter effects at 130 km are negligible Eq.(14) (Figure 5). The ambiguity coming from the choice θ_{23} or $\pi/2 - \theta_{23}$ is formally taken into account but has no effects in the results shown here, since the choice $\theta_{23} = 45°$ is made. A detailed discussion of the issues of degeneracies, correlations and clones is made in Section V.

In order to achieve the highest sensitivity it is clear that the systematic errors have to be kept at their lowest possible level. Such errors come essentially from the knowledge of the cross sections – which at the neutrino energies of the beta-beams (several hundred MeV) are not well known – as well as from the precision with which

all the other oscillation parameters are known, at the time such an experiment takes place. By placing a close detector of 1 kton at least at 1 km from the decay tunnel, one can exploit the same neutrino beams to perform precision cross section measurements (Mezzetto 2003). Note that, at the moment, the cross section uncertainty introduces variations in the sensitivities found in the literature. As far as the energy and the flux of the neutrino beams are concerned, one should keep in mind that contrary to conventional beams, in the case of beta-beams these are completely defined by the intensity of the ions and the kinematics Eqs.(16) and (17). The flux at the far detector is also completely determined by the divergence of the beam which is perfectly known. One can therefore hope to measure the signal and the backgrounds with a residual systematic error of 2 %. Figure 11 shows the importance of keeping the systematic errors at their lowest level.
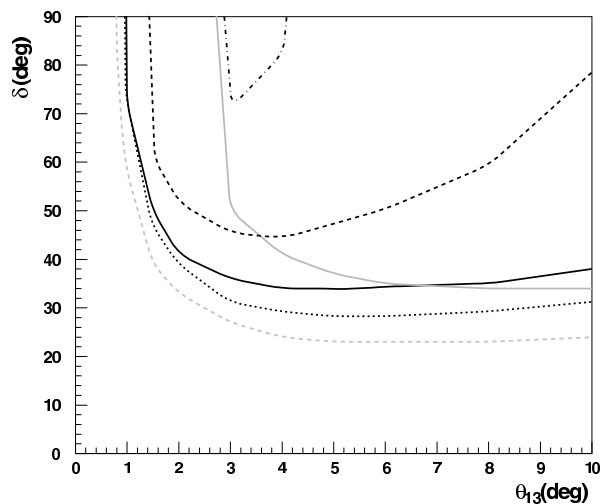

Figure 11. Discovery potential for δ at 3 σ, considering 10 years measurement time, with the two ions running at $\gamma = 60, 100$. The effect of systematic errors is shown. The curves correspond to 2 % (solid), 5 % (dashed), 10 % (dot-dashed) systematic errors. The results for a beta-beam with the two ions running at the same $\gamma = 75$ with 2 % systematic error is also shown (dotted). The two grey curves present the sensitivity of a super-beam (solid) and super-beam combined to a beta-beam (dashed) with 2 % systematic error (Mezzetto 2005a).

A different optimization of the ion acceleration can be obtained if each type of ion (either the ν_e or the $\bar{\nu}_e$ emitter) circulates separately at its optimal γ value, as suggested in (Mezzetto 2003, Burguet-Castell *et al* 2005, Lindroos 2005). In this case the single fluxes can be doubled by filling all the batches with the same type of ions (instead of alternating), which gives the same integrated number of decays per year. The physics potential obtained following such a prescription is studied with $\gamma(^6\text{He}) = \gamma(^{18}\text{Ne})=75$ in (Mezzetto 2003) and with $\gamma = 100$ (Figure 6) in (Mezzetto 2005b, Guglielmi *et al* 2005, Campagne *et al* 2006). These two choices well match the CERN-Fréjus distance of 130 km. The sensitivity on the third neutrino mixing angle as well as on the $\mathcal{CP}$ violating phase is presented in Figures 12 and 13 respectively, showing an increased discovery potential for both observables compared to the case where the two types of

ions circulate together in the storage ring. The beta-beam option alone is clearly a better strategy than a super-beam alone, as already apparent in Figures 9 and 11. Finally, the comparisons show that the largest discovery potential can be attained by a combination of a super-beam and a beta-beam.
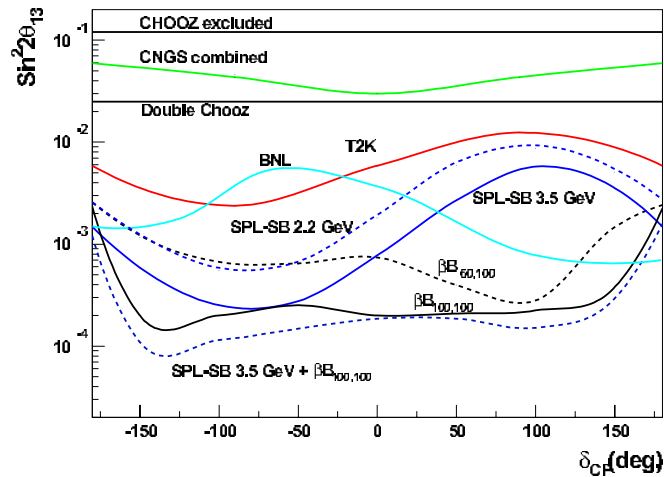

Figure 12. Sensitivity on the third neutrino mixing angle (90 % C.L.) as a function of the $\mathcal{CP}$ violating phase, with 2 % systematic errors, as in Figure 9. The discovery potential of Double CHOOZ (Ardellier *et al* 2004) is also presented. Here two different beta-beam options are compared, i.e. $\beta B_{60,100}$ and $\beta B_{100,100}$ where $\gamma(^6\text{He})=60$ and $\gamma(^{18}\text{Ne})=100$ and $\gamma(^6\text{He}) = \gamma(^{18}\text{Ne})=100$ are used respectively (Figure 6). The results correspond to 5 years ν_μ running time for the super-beam case (SPL-SB) with either 2.2 or 3.5 proton kinetic energy, and 5 years ν_e and $\bar{\nu}_e$ measurement time for the beta-beam case (Guglielmi *et al* 2005).
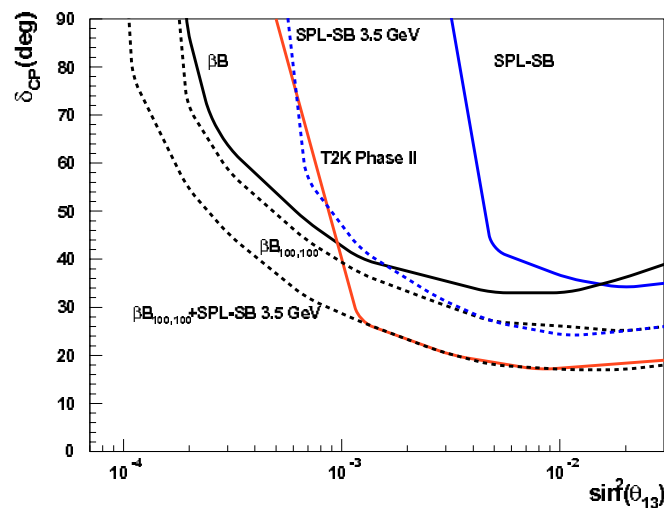

Figure 13. Same as Figure 12, but here all the results correspond to 10 years of data taking (Guglielmi *et al* 2005).

Since a beta-beam would exploit at most 10 % of the SPL protons (the injector), one could produce both a beta-beam and a super-beam and send these neutrino beams

to the same detector. This choice has several advantages. The use of the two beams does not only increase the statistics, but also gives the possibility to reduce the systematic errors and offers the necessary redundancy to firmly establish $\mathcal{CP}$ violating effects, within the reach of the experiments. Besides, the combination of a beta-beam and of a super-beam offers the largest discovery potential both with respect to the third mixing angle and to the $\mathcal{CP}$ violating phase. The last important advantage is that also $\mathcal{T}$ and $\mathcal{CPT}$ violation studies can be performed through a comparison of $\bar{\nu}_e \rightarrow \bar{\nu}_\mu$ oscillations (from beta-beams) to $\bar{\nu}_\mu \rightarrow \bar{\nu}_e$ Eq.(11) and to $\nu_\mu \rightarrow \nu_e$ Eq.(12) oscillations (from super-beams) respectively (Mezzetto 2003).

An extensive study of the beta-beam option at $\gamma = 100$ is made in (Campagne *et al* 2006) based on the GLoBES software (Huber *et al* 2005), including correlations and degeneracies (Section V) and using atmospheric data in the analysis (Huber *et al* 2005b). The GloBES software is a convenient tool to simulate long-baseline experiments and compare different facilities on the same footing. Correlations and degeneracies are fully taken into account letting all oscillations parameters to vary in the fits. A detailed comparison is made among the beta-beam, the super-beam (with 3.5 GeV proton kinetic energy), and T2K phase II (T2HK) facilities. The latter corresponds to the second phase of the T2K experiment in Japan, with a 4 MW proton driver and the Hyper-K detector located at 295 km (Itow *et al* 2001). It is a competing proposal with beta-beams with a similar size and timescale. In this work it is pointed out that if one assumes the $\mathcal{CPT}$ symmetry, a combination of a beta-beam and a super-beam sent at the same detector can be used to replace the anti-neutrino measurement by the $\mathcal{T}$ conjugate one. This implies that if both beams are available, the full information can be extracted with the neutrino beams only, reducing the 10 years measurement time down to 5. The corresponding sensitivity comes out to be very close to the 10 years measurement time with neutrinos and anti-neutrinos from one single experiment.

Figures 14 and 15 show the sensitivity on the third mixing angle and the discovery reach with respect to $\mathcal{CP}$ respectively. One can see that the three facilities have similar performances and can clearly reach values as small as $\sin^2 2\theta_{13} = 5\ 10^{-3}$, independently on δ. Besides, for a large fraction of δ values, a sensitivity of 10^{-3} can be attained. Assuming 2 % systematical error, in the best case $5(7)\ 10^{-3}$ can be reached for the beta-beam and T2HK (SPL). In a combined beta-beam and super-beam (SPL) experiment with 10 years measurement time $4\ 10^{-4}$ is reached for 45 % of δ values. Concerning $\mathcal{CP}$, the maximal violation corresponding to $\delta = \pi/2$ and $3\pi/2$ can be discovered down to $\sin^2 2\theta_{13} = 6(8)\ 10^{-4}$ (99 % C.L.) for the beta-beam (super-beam); while the best sensitivity is obtained for $\sin^2 2\theta_{13} > 10^{-2}$ since at this value $\mathcal{CP}$ violation can be established for 73 % (75 %) for all δ values with a beta-beam (super-beam). One can also see that the impact of systematical errors is crucial in the case of the T2HK experiment while the beta-beam and the SPL are much less sensitive. The comparison with T2HK shows that the $\gamma = 100$ beta-beam option has a very similar discovery reach and offers a competitive strategy for future neutrino precision oscillation measurements.

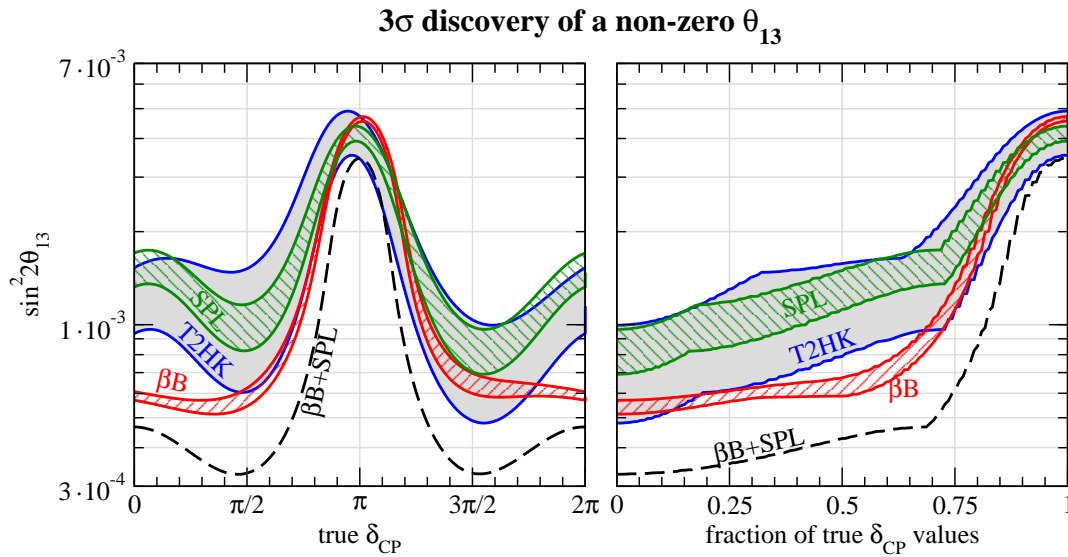Most of the literature concerning beta-beams considers the water Čerenkov

Figure 14. Sensitivity on θ_{13} at 3σ for the ($\gamma = 100$) beta-beam (βB), a super-beam (SPL), and T2HK (see text) as a function of the true value of δ_{CP} (left) and as a function of the fraction of all possible values of δ_{CP} (right). The width of the bands corresponds to values with 2% to 5% systematical errors. The dashed curves correspond to the combination of the beta-beam and the super-beam with 10 yrs measurement time each and 2% systematical error (Campagne *et al* 2006).

technique for the far detector. There are nowadays three proposal for very large water Čerenkov detectors: MEMPHYS in Europe (Mosca 2005a, Campagne *et al* 2006), UNO in the United States (Jung 2000) and HYPER-K in Japan (Itow *et al* 2001). This mature technology has already demonstrated excellent performances at the neutrino energies of several hundred MeV to 1 GeV. Other techniques are now being discussed, in particular the liquid Argon Time Projection Chamber (Rubbia C 1977, Rubbia A 2004, Ereditato and Rubbia 2004 and 2005), nuclear calorimetry and emulsions. It is important to emphasize that the large scale detector considered here can be exploited for a multidisciplinary program covering crucial issues in astrophysics, such as the detection of neutrinos from a(n) (extra-)galactic core-collapse Supernova, and in high energy physics, like proton decay. The field of neutrino astronomy has started with Davis' pioneering experiment (Davis 1964) which has measured solar neutrinos from the first time. Afterwards, neutrinos from a core-collapse Supernova have been observed during the explosion of the SN1987A, located in the Large Magellanic Cloud, at about 50 kpc from the Earth. For these important observations, both R. Davis and M. Koshiba received (with R. Giacconi) the Nobel Prize in 2002. Nowadays, neutrinos are currently used as a probe of astrophysical objects. In particular, the measurement of the neutrino lightcurve from a future core-collapse Supernova explosion constitute an essential ingredient to unravel the explosion mechanism, which keeps being a mystery: in the most recent tri-dimensional models the shock wave stalls and fails to eject the mantle. The neutrinos closely follow the explosion, from the collapse and the accretion phases, to the cooling of a proton-neutron star, or the formation of a black hole. Besides
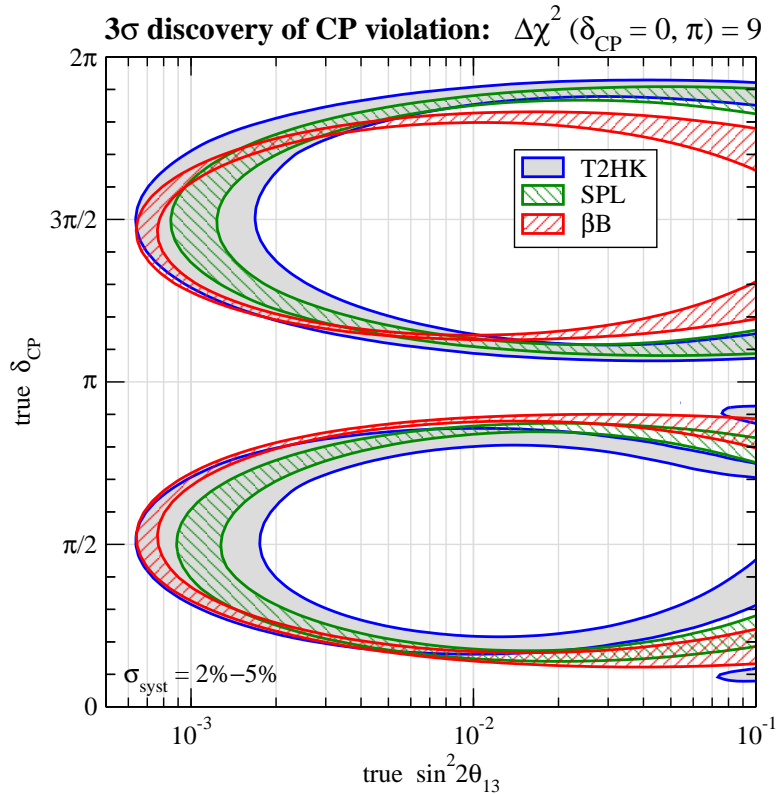
Figure 15. Same as Figure 14, but for the $\mathcal{CP}$ discovery reach. For parameter values inside the ellipse-shaped curves CP conserving values of δ_{CP} can be excluded at 3σ ($\Delta\chi^2 > 9$) (Campagne *et al* 2006).

a recently proposed technique, that consists in adding Gadolinium to a water Čerenkov detector (Beacom and Vagins 2004), can increase the sensitivity to the diffuse Supernova neutrino background from past Supernova explosions, for which there is at present an upper limit. The observation of both future and past Supernova neutrinos would bring invaluable information not only for our knowledge of Supernova physics, but also on neutrino properties which are still poorly known (Raffelt 1996, Fogli *et al* 2005). The water Čerenkov detector considered for the beta-beam project can measure about 150000 events from a Supernova at 10 kpc – while presently running detectors can observe at most 10000 events – and about 50 events from Andromeda. A flux of 250 events/10 years/500 kton from the diffuse background that can be increased by a factor of 10 with Gadolinium. Concerning proton decay one can attain a sensitivity up to 10^{35} years in the $e^+ \pi_0$ channel and a few 10^{34} years in the $K^+ \bar{\nu}$ channel (Jung 2000, Itow *et al* 2001, Mosca 2005a).

3. Low energy beta-beams

Very soon the idea of exploiting the beta-beam method to establish a facility that produces low energy neutrino beams – in the 100 MeV energy range – has been proposed, opening new axis of research in various domains of physics (Volpe 2004).

This corresponds to a range of about 7-14 for the ion boosts γ (Figure 7). The physics potential of such a facility is now being analyzed. Several applications have been studied concerning nuclear structure studies and neutrino-nucleus interactions (Volpe 2004, Serreau and Volpe 2004, McLaughlin 2004, Volpe 2005a), electroweak tests of the Standard Model (McLaughlin and Volpe 2004, Balantekin *et al* 2006a, Balantekin *et al* 2006b) as well as core-collapse Supernova physics (Volpe 2004, McLaughlin and Jachowitz 2005 and 2006). The physics case is also discussed in (Volpe 2005b, Volpe 2005c, Volpe 2006). A crucial outcome of (Serreau and Volpe 2004) is that a small devoted storage ring appears as more appropriate for low energy applications. The feasibility study of this storage ring (concerning e.g. size, ion intensities, stacking method, space charge effects) is now ongoing (Chancé and Payet 2005, Benedikt *et al* 2006). Here we summarize the status on the physics potential of low energy beta-beams‖.

3.1. Nuclear structure, neutrino-nucleus, nuclear astrophysics applications

In (Volpe 2004) it has been pointed out that the availability of neutrino beams in the 100 MeV energy range offers a unique opportunity to study spin-isospin and isospin nuclear excitations, for which nowadays little experimental information is available. Both the isospin and spin-isospin collective (and non-collective) modes are excited when a neutrino encounters a nucleus, due to the vector and axial-vector nature of the weak interaction. The (super-)allowed Fermi transitions – due to the vector current and therefore to the isospin operator – offer a well known example of such excitations at low momentum transfer. A precise knowledge of these nuclear transitions is essential for determining the unitarity of the CKM matrix, the analog of the MNSP matrix Eq.(9) in the quark sector (see e.g. Hardy and Towner 2005). Another less known but still intriguing example is furnished by the allowed Gamow-Teller transitions – due to the axial-vector current and therefore to the spin-isospin operator – in mirror nuclei, which are a tool for the search of the possible existence of second-class currents in the weak interaction (Weinberg 1958, Wilkinson 2000). These terms transform in an opposite way under the $\mathcal{G}-$ parity transformation¶ as the usual vector and axial-vector terms, and are not present in the Standard Model. Because of their importance, both the allowed Fermi and Gamow-Teller transitions have been studied for a very long time in nuclear physics through beta-decay and charge-exchange reactions (for the Gamow-Teller ones). While the precision achieved in the description of the (super-)allowed Fermi transitions is really impressive, our understanding of the allowed Gamow-Teller transitions still requires the use of an effective axial-vector coupling form factor, to take into account the "quenching" of the predicted transitions, compared to the ones measured in beta-

‖ Note that, after the proposals of pushing the ion Lorentz boosts to values higher than 60-100, the original scenario (Section II) is sometimes misleadingly referred to as "low energy" in the literature. The medium and high-energy scenarios are discussed in detail in Section IV.

¶ The $\mathcal{G}-$ parity transformation corresponds to the product of the charge-conjugation and of a rotation in isospin space.
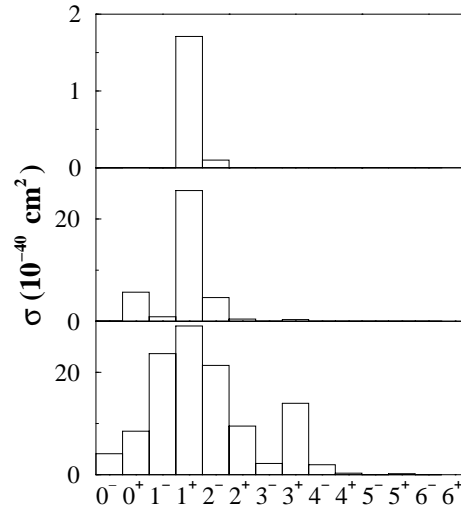
Figure 16. NUCLEAR STRUCTURE STUDIES WITH LOW ENERGY BETA-BEAMS: Contribution of isospin and spin-isospin nuclear states excited in the charged-current $^{208}\text{Pb}(\nu_e, e^-)^{208}\text{Bi}$ reaction (10^{-40} cm^2) for increasing neutrino energy, i.e. $E_{\nu_e} = 15$ MeV (up), 30 MeV (middle), 50 MeV (bottom). The histograms show the Isobaric Analogue State ($J^\pi = 0^+$), the allowed Gamow-Teller ($J^\pi = 1^+$), the spin-dipole ($J^\pi = 0^-, 1^-, 2^-$), as well as states of higher multipolarity ($J^\pi = 2^+, 3^-, 3^+, 4^-, 4^+$). For the latter no experimental information is available. Their contribution to the total cross section becomes significant when the impinging neutrino energy increases (Volpe 2004).

decay or charge-exchange reactions (see for example Osterfeld 1992). The still open "quenching" problem represents a limitation in our description of the weak spin-isospin nuclear response, in spite of the crucial role that it plays in various hot issues in nuclear astrophysics and in high energy physics.

Little or no experimental information is available for the spin-isospin and isospin nuclear excitations such as the spin-dipole ($J^\pi = 0^-, 1^-, 2^-$), or the states of higher multipolarity (e.g. $J^\pi = 2^+, 3^-, 3^+, 4^-, 4^+$). These states come into play when a weak probe transfers a finite momentum to a nucleus, like in muon capture or in neutrino-nucleus interactions. Supplementary information on the corresponding weak transition amplitudes can be furnished by electron scattering studies, which however explore nuclear excitations induced by the vector current only. As an illustrative example Fig.16 shows the contribution of spin-sospin and isospin transitions excited in neutrino scattering on lead, and their evolution when the neutrino energy increases. A quantitative estimate of the importance of such states is also gathered by computing the flux-averaged cross sections[+], which are the relevant quantities for experiments. If one considers the neutrino fluxes corresponding to the decay-at-rest of muons, the spin-dipole states ($J^\pi = 0^-, 1^-, 2^-$) contribute by about 40 % in ^{12}C (Volpe *et al* 2000) and ^{56}Fe (Kolbe and Langanke 2001), and by about 68 % in ^{208}Pb (Volpe *et al* 2002).

[+] Flux-averaged cross sections are obtained by folding the cross sections with the neutrino flux of the source.

The contribution from the states of higher multipolarity is about 5 % and 25 % in iron and lead respectively; while it amounts to about 30 % in carbon (Volpe *et al* 2000) and 60 % in lead (Volpe *et al* 2002) if neutrinos are produced from pion decay-in-flight. Since low energy beta-beams have the specificity that the average neutrino energy can be increased by increasing the Lorentz boost of the ions, they constitute a promising tool for the study of these states, through a systematic study on various nuclear targets and different neutrino energies. Even though the measured cross sections are, in the majority of cases, inclusive, experimental information on these states can be extracted by changing the Lorentz ion boosts since different pieces of the nuclear response are important at different energies (Volpe 2004, Figure 16).

A facility based on conventional sources (decay of pions and muons) offers another possible strategy to dispose of low energy neutrinos beams (Avignone F T *et al* 2000, Efremenko 2004). The first feasibility studies show that the neutrino intensities are expected to be higher with conventional sources than with beta-beams. On the other hand, the neutrino beams obtained with the two options present complementary features, both for the flavour content and for the energy. Conventional sources provide us with neutrinos of different flavours and a Michel spectrum (from muon decay-at-rest) peaked at about 35 MeV and with 53.8 MeV maximum energy. Beta-beams are pure in flavour and have the important advantage that the neutrino energy can be tuned by varying the acceleration of the ions. This is a particularly important feature for extracting nuclear structure information, as discussed above. In (McLaughlin 2004) neutrino scattering on lead is taken as an example to show another procedure to extract information on the different spin-isospin and isospin excitations, namely through a comparison of measurements with conventional beams and low energy beta-beams (Figure 17). In fact, the corresponding neutrino fluxes are in the same energy range for $\gamma = 7$, but their shape and average energies are different. Besides, the measurement of the cross section without or with (one or two) neutrons can be used for the same purpose, in the specific case of the lead nucleus (McLaughlin 2004).

A better knowledge of the weak nuclear response can have a broad impact, since neutrino-nucleus interactions represent a topic of current great interest for neutrino physics and nuclear astrophysics. The motivations come from the need for a precise knowledge of neutrino detector responses, both in neutrino experiments and in core-collapse Supernovae observatories, and also from open issues in core-collapse Supernovae physics, such as unraveling the site for the nucleosynthesis of heavy elements (McLaughlin and Fuller 1995, Haxton *et al* 1997, Qian *et al* 1997, Borzov and Goriely 2000, Balantekin and Fuller 2003,Terasawa *et al* 2004). or from neutrino-nucleosynthesis (Woosley *et al* 1990, Heger *et al* 2003, Haxton 2004, Langanke and Pinedo 2004). However, the available experimental neutrino-nucleus scattering data in the relevant energy range is limited, since deuteron, carbon and iron are the only nuclei investigated so far. As a consequence one has to rely on the numerous theoretical predictions and on extrapolations to the nuclei and energies of interest. These calculations exploit a variety of approaches, among which Effective Field Theories, the Shell Model and
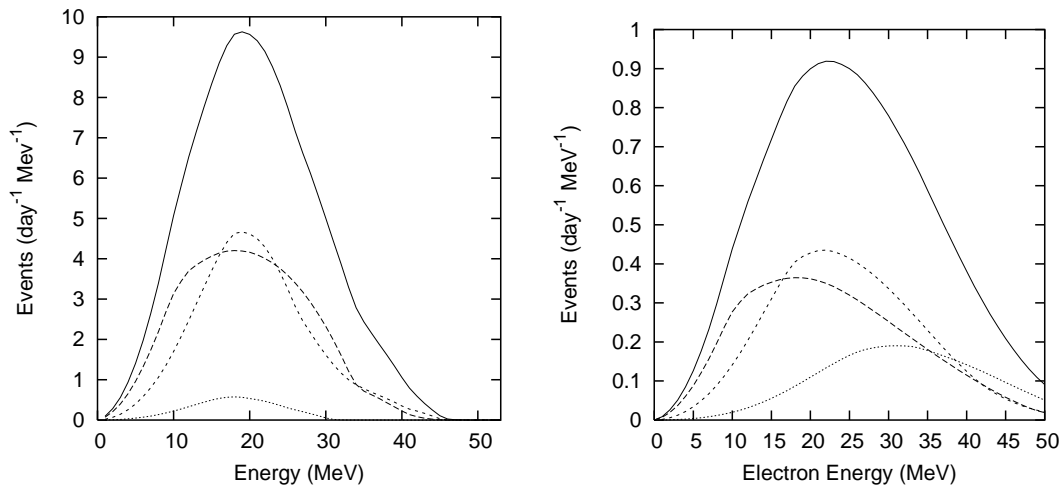
Figure 17. Total electron spectrum coming from charged current neutrino scattering on lead (solid line), with neutrinos coming from pion decay-at-rest (left) and from low energy beta-beams with $\gamma = 10$ (right). The other curves present the contribution from the allowed Fermi and Gamow-Teller states (long dashed line), from the $0^-, 1^-, 2^-$ and the $2^+, 3^-, 3^+, 4^-, 4^+$ states (dotted line) (McLaughlin 2004).

the Random-Phase-Approximation, and the Elementary Particle Model (Kubodera and Nozawa 1994, Kolbe *et al* 2003). The cross sections estimates agree quite well at very low energies, where the nuclear response is dominated by the allowed Fermi and Gamow-Teller transitions. However, important discrepancies appear at higher neutrino energies, when the other nuclear excitations become important (Figures 16 and 17). In this energy region, the calculations are in fact largely subject to nuclear structure uncertainties and model dependencies (e.g. treatment of the continuum, choice of the forces, higher-order correlations). The present discrepancies between the predicted and measured neutrino-carbon cross sections and between the calculations in the case of lead are talkative examples (Volpe 2005c) of the difficult theoretical task. Systematic neutrino-nucleus interaction studies performed with low energy beta-beams offer a perfect tool to explore the nuclear response in this energy region in great detail, and put the theoretical predictions on a firm ground.

The number of neutrino-nucleus scatterings expected at a low energy beta-beam facility has been calculated in (Serreau and Volpe 2004). The effects of the geometry of the storage ring has in particular been analyzed. Two sizes are considered: the one from the original scenario (Figure 8) and a small storage ring, as the one envisaged for the future GSI facility (see GSI). The results of exact numerical calculations using Eqs.(14-20) are shown in Table 3 for several target nuclei. The detectors are those considered for the ORLAND facility (Avignone F T *et al* 2000). An analytical formula is derived to scale the rates in Table 3 to different storage ring sizes. Note that for a close detector, due to the flux anisotropy, the rates do not simply scale as S/D, as in the case of a far detector (like those considered in Sections II, IV and VI). It is clear that interesting neutrino-nucleus rates can be attained at such a facility. A crucial outcome of (Serreau and Volpe 2004) is that a small devoted storage ring is much more favorable for low

Table 3. Neutrino-nucleus interaction rates at a low energy beta-beam facility ($\gamma = 7 - 14$): The expected events per year (3.2×10^7 s) on several target nuclei obtained for $\gamma = 14$ with Eqs.(14-20) are presented. The effect of the storage ring geometry is shown (S and D are the total and straight section lengths respectively). The detectors are located at 10 meters from the storage ring and have cylindrical shapes (R=1.5 m and h=4.5 m for deuteron, iron and lead, R=4.5 m and h= 15 m for oxygen, where R is the radius and h is the depth of the detector). Their mass is indicated in the second column (Serreau and Volpe 2004).

Reaction	Mass (tons)	Small Ring (S=450 m, D= 150 m)	Large Ring (S=7 km, D=2.5 km)
ν+D	35	2363	180
$\bar{\nu}$+D	35	25779	1956
ν+^{16}O	952	6054	734
$\bar{\nu}$+^{16}O	952	82645	9453
ν+^{56}Fe	250	20768	1611
ν+^{208}Pb	360	103707	7922

energy applications. The physical reason is simple. The flux emittance is large because of the very low γ values: only the ions which decay close to the detector contribute to the rates. The feasibility study of the small storage ring is now ongoing (Benedikt *et al* 2006).

A novel procedure to determine the response of a target nucleus in a supernova neutrino detector directly, through the use of low energy beta-beams, is pointed out in (Jachowicz and McLaughlin 2005 and 2006). It is shown that the cross sections folded with a supernova neutrino spectrum can be well reproduced by linear combinations of beta-beam spectra. This comparison offers a direct way to extract the main parameters of the supernova neutrino flux. The proposed procedure appears quite stable against uncertainties coming from the experiment, or the knowledge of the cross section, that give rise to a "noise" in the expansion parameters.

Finally, it has been recently pointed out (Volpe 2005a) that neutrino-nucleus interactions are also important for the search of neutrinoless double-beta decay in nuclei. In fact, by rewriting the neutrino exchange potential in momentum space and by using a multiple decomposition, the two-body transition operators, involved in the former, can be rewritten as a product of the one-body operators involved in neutrino-nucleus interactions (except for the short range correlations as well as possible phases present in the two-body process). Neutrino-nucleus scattering data offer a potential new constraint for the predictions on the neutrinoless double-beta decay half-lives. At present these calculations suffer of important discrepancies for the same candidate nucleus. Beta-decay (Muto *et al* 1989, Aunola and Suhonen 1996), muon capture (Kortelainen and Suhonen 2002 and 2004), charge-exchange reactions (Akimune 1997, Bernabeu *et al* 1988) and double-beta decay with the emission of two neutrinos (Rodin *et al* 2003) have used to constrain the calculations so far. Neutrino-nucleus measurements would

have the advantage that, if both neutrinos and anti-neutrinos are available, the nuclear matrix elements involved in the two branches of neutrinoless double-beta decay – from the initial and the final nucleus to the intermediate one – can be explored.

3.2. Fundamental interaction studies

Three applications for fundamental interaction studies have been discussed so far: the measurement of the Weinberg angle at low momentum transfer (Balantekin *et al* 2006a), a CVC test with neutrino beams (Balantekin *et al* 2006b) and a measurement of the neutrino magnetic moment (McLaughlin and Volpe 2004). The measurement of the Weinberg angle represent an important test of the electroweak theory. Several experiments at different Q^2 exist, namely the atomic parity violation (Bennett and Wieman 1999) and Moller scattering at $Q^2 = 0.026$ GeV^2 (Anthony *et al* 2005) which combined with the measurements of $\sin^2 \theta_W$ at the Z^0 pole (ALEPH *et al* 2005), are consistent with the expected running of the weak mixing angle. However, recent measurement of the neutral- to charged-current ratio in muon anti-neutrino-nucleon scattering at the NuTEV experiment disagrees with these results by about 3 σ (Zeller *et al* 2002). A number of ideas were put forward to explain the so-called NuTEV anomaly (Davidson *et al* 2001, Loinaz *et al* 2004, Miller and Thomas 2005, Giunti and Laveder 2002). However, a complete understanding of the physics behind the NuTEV anomaly is still lacking; probing the Weinberg angle through additional experiments with different systematic errors would be very useful. The possibility of using a low energy beta-beam facility to carry out such a test with neutrino-electron scattering at low momentum transfer, i.e. $Q^2 = 10^{-4}$ GeV^2 is investigated in (Balantekin *et al* 2006a). In particular it is shown that since the neutrino flux and average energy are well known in the case of beta-beams, the number of counts is in principle sufficient to extract information on the Weinberg angle. A fully efficient 1 kton Čerenkov detector is located at 10 meters from a small storage ring having 1885 m total length and 678 m straight sections, in which the expected intensities for $\gamma = 7 - 14$ are 0.5 10^{11} helium-6/s and 2.7 10^{12} neon-18/s (while the intensities at production are the same as in Table 1). These numbers are the outcome of a preliminary feasibility study of the small storage ring (Chancé and Payet 2005). The (anti)neutrino on electron events are identified by an angular cut. The background from neutrino-proton scattering is suppressed by the use of Gadolinium (Beacom and Vagins 2004). Figure 18 shows the improved precision one gets by combining measurements with different gamma values. The results corresponds to one (3x10^7 s) year measurement at each gamma and a purely statistical total count error. Figure 19 shows the precision with which the Weinberg angle can be measured after the inclusion of both statistical and systematic errors. In particular, if the systematic error can be kept below 10 %, a precision of 10 % seems to be within reach at a beta-beam facility.

The CVC hypothesis connects weak and electromagnetic hadronic currents. Several tests of CVC have been performed in the past (see e.g. Thomas 1996), concerning, in particular, the vector form factor, through super-allowed nuclear beta-decays studies
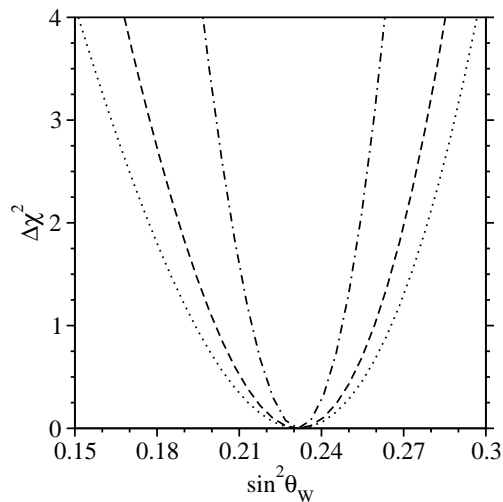
Figure 18. A WEINBERG ANGLE MEASUREMENT WITH LOW ENERGY BETA-BEAMS: $\Delta\chi^2$ with $\gamma = 12$ (dotted line), with $\gamma = 7, 12$ (broken line), and with $\gamma = 7, 8, 9, 10, 11, 12$ (dash-dotted line). The results were obtained considering a one year (3×10^7 s) measurement duration at each γ, and for a helium-6 intensity at the storage ring of 2.7×10^{12} ions/s (Chancé and Payet 2005). The count number error was considered to be purely statistical. The 1σ ($\Delta\chi^2 = 1$) relative uncertainty in the Weinberg angle is 15.2% for $\gamma = 12$, 12.3% for $\gamma = 7, 12$, and 7.1% for $\gamma = 7, 8, 9, 10, 11, 12$ (Balantekin *et al* 2006a).
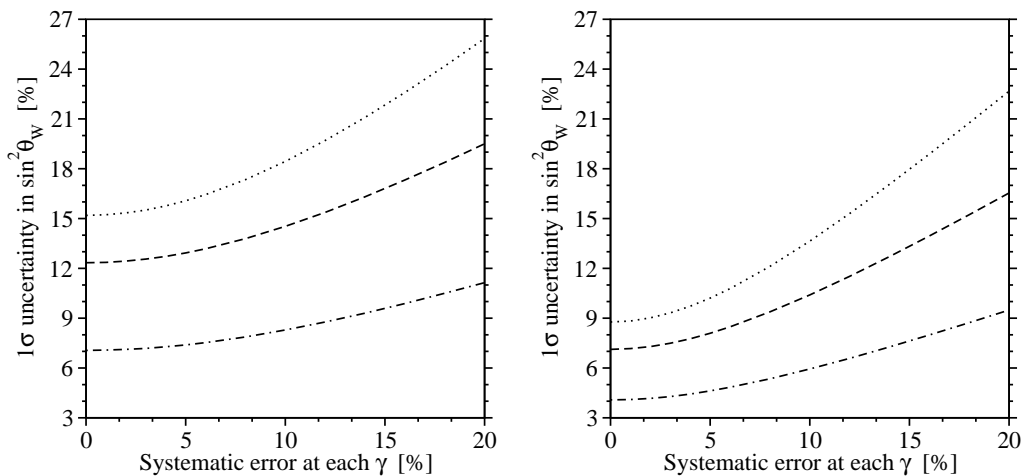

Figure 19. One sigma uncertainty in the Weinberg angle as a function of the systematic error at each γ for $\gamma = 12$ (dotted line), for $\gamma = 7, 12$ (broken line), and for $\gamma = 7, 8, 9, 10, 11, 12$ (dash-dotted line). The helium-6 intensity at the storage ring is 2.7×10^{12} ions/s on the left panel (Chancé and Payet 2005), and with an increased intensity of 8.1×10^{12} ions/s on the right panel. In both cases, the measurement duration at each γ is one year (3×10^7 s) (Balantekin *et al* 2006a).
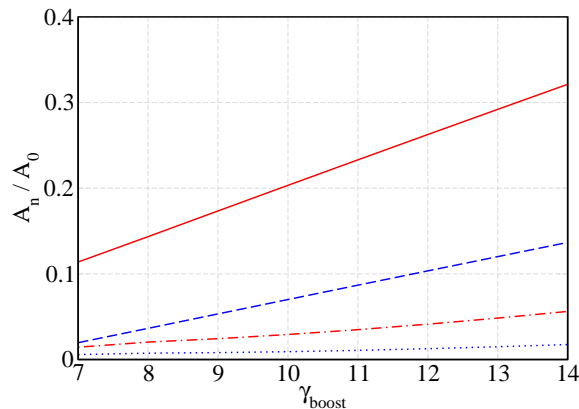
Figure 20. A CVC TEST: The $\bar{\nu}_e + p \rightarrow e^+ + n$ reaction is used to test the weak magnetism form factor using neutrinos from low energy beta-beams and a water Čerenkov detector. The figure shows the ratio of the first (A_1) and second (A_2) order Legendre polynomial coefficients to the zeroth order one (A_0, the number of events) as a function of the ion Lorentz boost. These expansion coefficients determine the angular distribution of the emitted positrons with (solid is for A_1/A_0; dash-dotted is for A_2/A_0) and without (dashed is for A_1/A_0; dotted is for A_2/A_0) the weak magnetism term. The overall effect of the weak magnetism term on the angular distribution is considerably larger than on the total number of events and increases with the Lorentz ion boost. Note that when the weak magnetism is considered, its value is set to its CVC value (Balantekin *et al* 2006b).

(see e.g. Hardy and Towner 2004). Verifying that the CVC hypothesis correctly predicts tensor terms – often referred to as weak magnetism – is of fundamental importance (Deutsch *et al* 1977). So far, this contribution to the weak currents has been tested in an experiment involving the beta-decay of Gamow-Teller transitions in mirror nuclei in the A=12 triad (Lee *et al* 1963, Wu 1964, Lee and Wu 1965). A test based on neutrino-nucleon collisions at low momentum using low energy beta-beams is proposed in (Balantekin *et al* 2006b). This would have, in particular, the advantage that there is no uncertainty coming from nuclear structure calculations. It is important to keep in mind in that, in addition to providing important tests of the Standard Model, neutrino-nucleon reactions play a crucial role in understanding the dynamics of the core-collapse supernovae (Balantekin and Fuller 2003, Horowitz 2001), the yields of the r-process nucleosynthesis that could take place in such environments (Meyer *et al* 1998) and also contribute to the energy transfer (from the accretion-disk neutrinos to the nucleons) in gamma-ray bursts models (Ruffert *et al* 1996, Kneller *et al* 2004). Finally, understanding the subtleties of the neutrino-nucleon interactions are crucial to the terrestrial observation of neutrino signals (Vogel and Beacom 1999, Beacom *et al* 2002). In (Balantekin *et al* 2006b) the sensitivity to the weak magnetism term that can be achieved in the $\bar{\nu}_e + p \rightarrow e^+ + n$ reaction, both with the total number of events and with the angular distribution of the emitted positrons, is studied. For this purpose the same setup, as for the measurement of the Weinberg angle is taken, and the interaction of anti-neutrinos on protons in a water Čerenkov detector is considered.
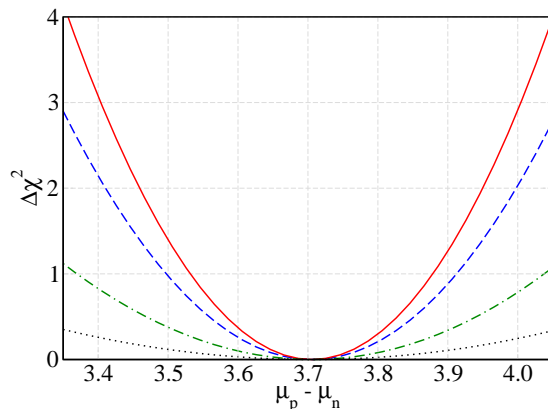
Figure 21. Same as for the previous Figure, but for $\Delta\chi^2$ obtained from the angular distribution of events (see text) in the cases when the total error is purely statistical (solid), and when one includes 2% (dashed), 5% (dash-dotted) and 10% (dotted) systematic errors. The 1σ ($\Delta\chi^2 = 1$) relative uncertainty in $\mu_p - \mu_n$ is 4.7%, 5.6%, 9.0% and more than 20%, respectively. These results were obtained considering $\gamma = 12$ (Balantekin *et al* 2006b).

The angular distribution can be expanded in Legendre polynomials whose coefficients are shown in Figure 20 (left), as a function of the Lorentz ion boost. While the zeroth order coefficient is nothing but the total number of events, the first order measures the strength of a linear term which favors forward peaked events. The results show that, when systematic errors are taken into account, the angular distribution is a much better tool than the total number of events to extract information on the weak magnetism form factor (Figure 20 right). In particular, if those errors are kept below 5 %, a one year measurement of the weak magnetism is possible at a 1 σ level of 9 %, if the ions in the storage ring are boosted to $\gamma = 12$. An even better measurement is expected if the ions are boosted to $\gamma's$ larger than 12, because of the increasing importance of the weak magnetism contribution with the impinging neutrino energy. This way of probing the weak magnetism form factor at low momentum transfer constitutes a new test of the Conserved Vector Current Hypothesis.

It is interesting to note that one might use the ion decay at rest as an intense neutrino source, in order to explore neutrino properties that are still poorly known, such as the neutrino magnetic moment (McLaughlin and Volpe 2004). Direct measurements to achieve improved limits are precious, since the observation of a large magnetic moment points to physics beyond the Standard Model. Note that such an application does not require any acceleration of the ions. Once produced, the ions are fired to a target inside a 4π detector. The measurement of the (anti)neutrino interaction with the electrons, as a function of the electron recoil, is then used to set limits on the neutrino magnetic moment. Current bounds come from direct measurements using reactor neutrinos, and are in the range $\mu_\nu < 1.0 - 4 \times 10^{-10}\mu_B$ (Daraktchieva *et al* 2003, Li *et al* 2003, Reines *et al* 1976, Vogel and Engel 1989, Vidyakin *et al* 1992, Derbin *et al* 1993). From
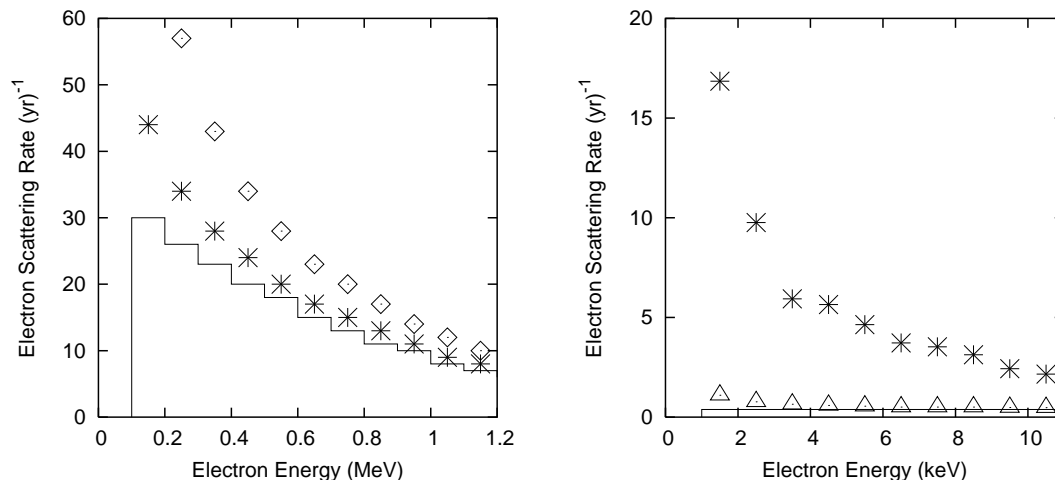
Figure 22. MEASUREMENT OF THE NEUTRINO MAGNETIC MOMENT WITH
LOW ENERGY BETA-BEAMS: Number of neutrino-electron scattering events
from helium-6 ions, produced at the rate 10^{15} per second, and sent inside a
4π detector of 10 m in radius. Similar results are obtained with neon-18 ions.
(Note that for this application ion acceleration is not needed.) The symbols
show the number of scatterings if the neutrino has a magnetic moment of
$\mu_\nu = 10^{-10}\mu_B$ (diamonds), $\mu_\nu = 5 \times 10^{-11}\mu_B$ (stars) and $\mu_\nu = 10^{-11}\mu_B$
(triangles). The histogram shows the results for a vanishing neutrino magnetic
moment (McLaughlin and Volpe 2004).

solar neutrino-electron scattering at Super-Kamiokande a limit of $< 1.5 \times 10^{-10}\mu_B$ at
90 % C.L. has been obtained (Beacom and Vogel 1999). Upper limits in the range
$10^{-11} - 10^{-12}\mu_B$ are also inferred, from astrophysical and cosmological considerations
(Raffelt 1996), the exact values being model dependent. The prospects from using low
energy beta-beams to improve the direct bounds has been studied in comparison with
reactor neutrinos and a very intense tritium source (McLaughlin and Volpe 2004). While
the advantage of using beta-beams is that the neutrino flux is perfectly known, the main
limitation for this application is clearly the intensity of the ions. Figure 22 shows the
electron-neutrino scattering events in the range of 0.1 MeV to 1 MeV and 1 keV to 10
keV respectively. The results shown are obtained for an (increased) intensity of 10^{15} ν/s
(i.e. 10^{15} ions/s). If there is no magnetic moment, this intensity produces about 170
events in the 0.1 MeV to 1 MeV range per year and 3 events in the 1 keV to 10 keV
range per year. These numbers increase to 210 and 55 respectively in the case of a
magnetic moment of $5 \times 10^{-11}\mu_B$. In conclusion, by measuring electron recoils in the
keV range with a beta-beam source one can, with a sufficiently strong source, have a
very clear signature for a neutrino magnetic moment of few $10^{-11}\mu_B$. A detailed study
of the background, at these small electron recoil energies, and a precise knowledge of
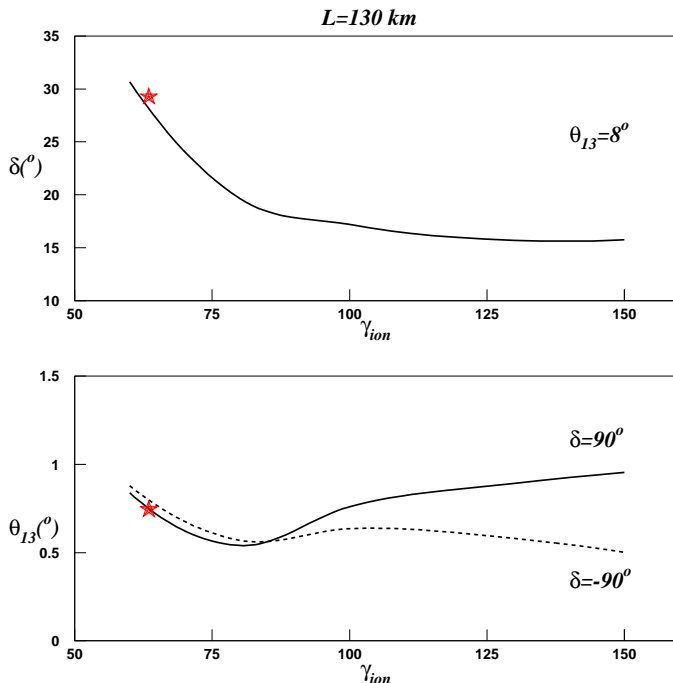the ion-induced background, are now needed.

Figure 23. Sensitivity curves (99 % C.L.) for δ (upper) and θ_{13} (lower), as a function of the ion boost. The CERN-Fréjus baseline with a 440 kt water Čerenkov detector are considered. The (anti)neutrino emitters run at the same gamma. The stars present the results obtained for the original option where the ions run at $\gamma = 60, 100$ (Section II) (Burguet-Castell *et al* 2005).

4. Medium and high energy scenarios

The idea of pushing the Lorentz ion boosts to higher values than the ones proposed in the original scenario (Zucchelli 2002) is first proposed in (Burguet-Castell *et al* 2004). In particular, the sensitivity to $\mathcal{CP}$ violation of the original scenario (Section II) is compared to two new baselines where the ions are accelerated at either $\gamma = 350/580$ for helium-6/neon-18, and sent to a distance of $L = 720$ km, or at $\gamma = 1500/2500$ and sent to $L = 3000$ km. The former case would require a refurbished SPS to reach such accelerations at CERN, while the water Čerenkov detector detector could, for example, be located at the Gran Sasso Laboratory. The latter case would necessary need something like LHC and a baseline such as the CERN-Canary islands with e.g. a 40 kton tracking calorimeter. If the baseline is adjusted appropriately one can remain close to the atmospheric oscillation maximum. Working at higher boosts has essentially two advantages. The appearance oscillation signal increases linearly with gamma (and then saturates for $\gamma \approx 400$ in a water detector), which results in a gain in sensitivity. Besides, some ambiguities on the neutrino parameters due to the degeneracies can be disentangled, both by using the neutrino energy reconstruction in the detector, and by
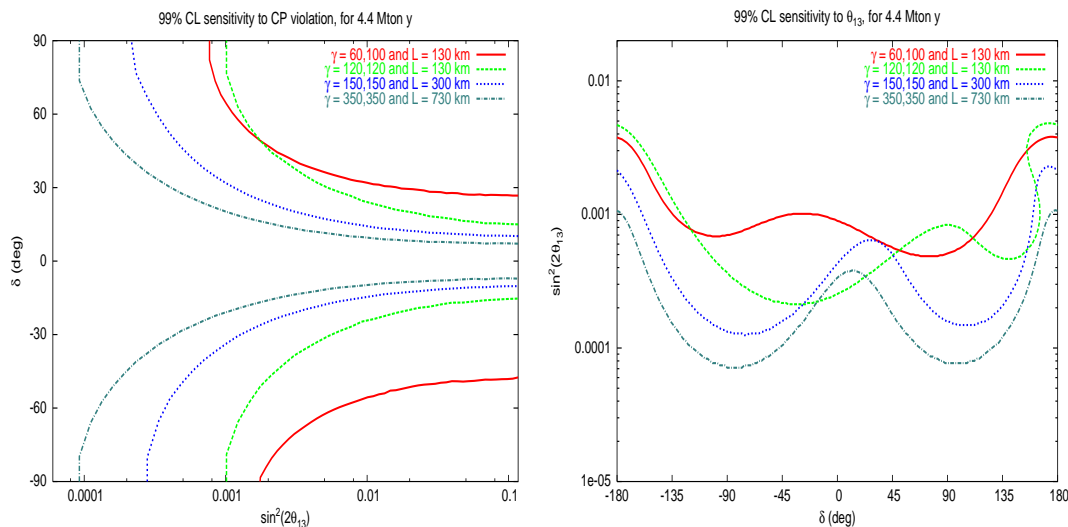
Figure 24. Exclusion plots (99 % C.L.) for δ (left) and θ_{13} (right) for the original scenario in comparison with the options $\gamma = 120, 150, 350$ and $L = 130, 300, 730$ km for the source-detector distance, respectively. The solar and atmospheric oscillation parameters are fixed to the present best values (Burguet-Castell *et al* 2005).

exploiting matter effects (that become significant for baselines of $O(1000)$ km, Figure 5). Ref.(Burguet-Castell *et al* 2004) has triggered a number of studies (Terranova *et al* 2004, Burguet-Castell *et al* 2005b, Huber *et al* 2005, Agarwalla *et al* 2005). The medium and high energy options have also been discussed in (Terranova 2005, Gomez-Cadenas 2005, Migliozzi 2005). In (Donini *et al* 2005a) the medium γ (350-580) case is analyzed exploiting a CERN-Gran Sasso Laboratory baseline with a non-magnetized iron detector. It is shown that the $\mathcal{CP}$ violating phase can be determined down to 30° (99 % C.L.), if $\theta_{13} > 3$°. In (Agarwalla *et al* 2005) the high energy option is discussed with a baseline from CERN to Rammam or Singara where an iron calorimeter detector could be located. Performances can be found in the literature for $\gamma = 150$ (Burguet-Castell *et al* 2005), 200 (Huber *et al* 2005a), 350 (Burguet-Castell *et al* 2005), 500 (Huber *et al* 2005a, Terranova *et al* 2004), 1000 (Huber *et al* 2005a), 2000 (Burguet-Castell *et al* 2004) and 2488 (Terranova *et al* 2004).

In (Burguet-Castell *et al* 2005) a detailed analysis of the sensitivity with a Lorentz ion boost of $\gamma = 150$ is made. This choice corresponds to the maximum acceleration that can be achieved using the existing CERN-SPS (Lindroos 2005). In particular, the following three issues are addressed: *i)* a sensitivity study of the CERN-Fréjus baseline with a megaton water Čerenkov detector and $\gamma \geq 100$; *ii)* the optimal baseline at this γ and with such setup; *iii)* the (dis)advantages of using different values of γ for the (anti)neutrino emitters. The intensities used are the same as in the original scenario, namely 2.9×10^{18} ^{6}He and 1.1×10^{18} ^{18}Ne, while the measurement period is 10 years. Note that the water Čerenkov detector considered is suitable for quasi-elastic events. Therefore the sensitivity improves until the inelastic cross section starts to dominate
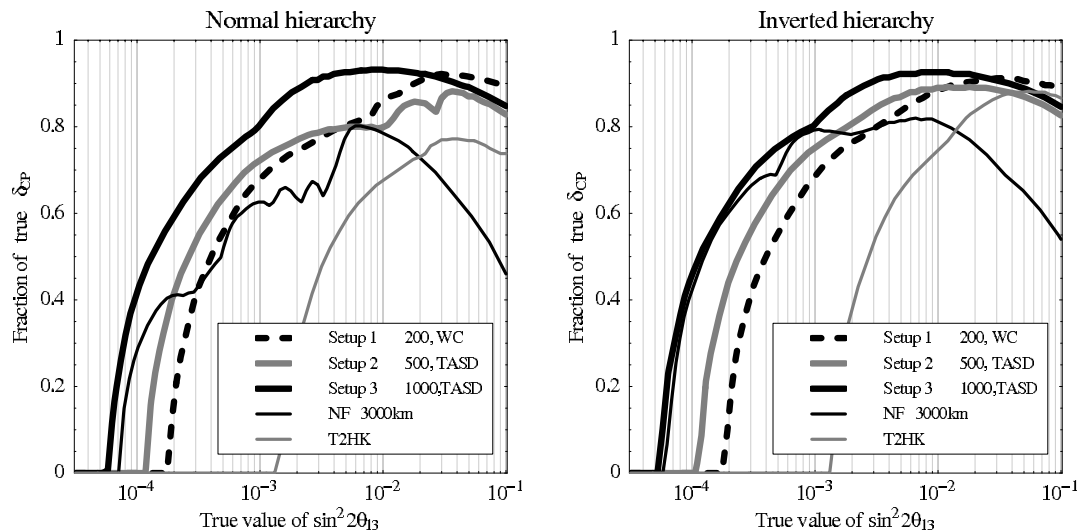
Figure 25. The figure shows a comparison of the $\mathcal{CP}$ violation sensitivity for the normal (left) and inverted (right) mass hierarchy as a function of the true values for $\sin^2\theta_{13}$ and δ_{CP} at the 3 σ C.L. A comparison is made between beta-beams with different ion boosts and detector technologies (WC and TASD) on one hand, and neutrino factories (NF@3000 km) and super-beams (T2HK) on the other hand. On the y-axis is shown the values of δ_{CP} "stacked" to the $\mathcal{CP}$ fraction (Huber *et al* 2006).

(for $\gamma \geq 400$). The angular and energy cuts as well as the time structure of the ion bunches help keeping the atmospheric background at a very low level, while the beam-induced neutral current single-pion production, that can mimic the appearance signal, is manageable even for $\gamma = 100$.

Figure 23 shows the sensitivity on δ and θ_{13} as a function of the ion boost for the CERN-Fréjus baseline. It is clearly seen that by using $\gamma = 100$ the increased event rates imply a definite gain in the δ sensitivity compared to the lower gamma values first envisaged, while its behavior keeps rather flat in the range 100-150 (since for these cases the neutrino flux at lower energies contributing to the event rate is practically the same). The study of the optimal source-detector L distance, for the maximum SPS ion acceleration of 150, points to $L = 300$ km, i.e. the distance corresponding to the first atmospheric neutrino oscillation maximum.

A comparison of the δ and θ_{13} exclusion plots for the original scenario, the $\gamma = 120, 150$ with $L = 130, 300$ km, and 350 with and 730 km from (Burguet-Castell *et al* 2004), is presented in Figure 24. Note that the energy dependence of the signal can be well reconstructed since the neutrino energies are above the Fermi momentum of the target nuclei (this is not the case for the original scenario). This information can be used at $\gamma = 150$ (350) and $L = 300$ (700) to resolve the intrinsic degeneracies. A major issue for such a baseline is to find a location to house the detector, the Canfranc Underground Laboratory being now discussed as a possible option.

An interesting and detailed analysis of the $\mathcal{CP}$ violation sensitivity is made in (Huber *et al* 2006), for Lorentz ion boosts values ranging from 100 to 3000. Note that
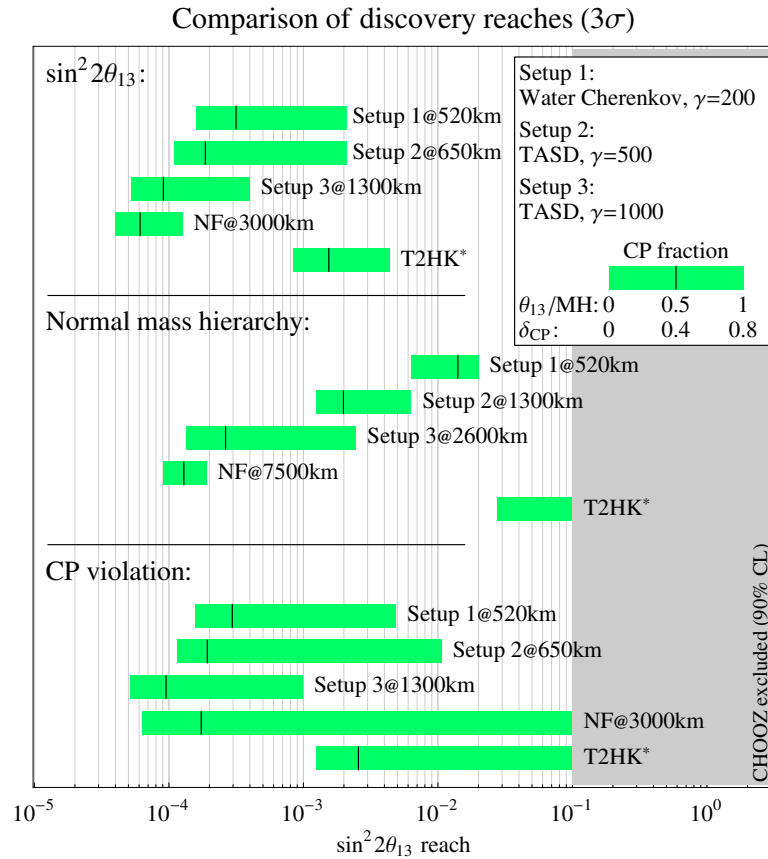
Figure 26. A comparison of the discovery reach at the 3σ confidence level. The bars represent the best case (left end), "typical case" (middle line), and worst case (right end) in δ_{CP}, where the respective sensitivities are computed with the CP fractions in the plot legend. Note that for CP violation, a CP fraction of one can never be achieved since values close to 0 or π cannot be distinguished from CP conservation. Within each category, the most competitive setups from this study are compared. For all shown sensitivities, a normal mass hierarchy is assumed (Huber *et al* 2006).

here the performance at high gammas is studied considering that the intensities are reduced (and not constant as in previous studies) for very high gammas. While a 500 kt water Čerenkov detector is considered for a boost of 200, a 50 kt totally active scintillator detector (TASD) is taken for higher ion accelerations. The whole study is performed by using the GLoBES software (Huber *et al* 2005) which allows, in particular, to include degeneracies and correlations (see Section V). A detailed comparison with neutrino factories with a 50 kt magnetized iron detector and very intense super-beams (as those that will be available at T2HK) is made (Figure 25). Figure 26 presents the main results of this work as far as the third neutrino mixing angle, the Dirac phase and the normal mass hierarchy are concerned. One can see the excellent performance of the $\gamma = 200$ setup compared both to super-beams and to neutrino factories. Such a discovery reach is achieved by including the second oscillation maximum to disentangle correlations and degeneracies. This also depends on the choice of approximately equal neutrino and

anti-neutrino event rates for all setups. On the other hand the higher gammas appear as competitive options to a neutrino factory. In conclusion, the discovery reach for $\gamma > 150$ is very promising as well. However, at least for the moment, it remains more speculative, since it is neither based on an existing accelerator complex nor on a robust estimation of the ion intensities. These scenarios clearly deserve further investigations.

5. The issue of the degeneracies

A characteristic feature in the analysis of future neutrino accelerator experiments is the presence of the so-called "parameter degeneracies", which is the appearance of various disconnected regions in the multi-dimensional oscillation parameter space, besides those corresponding to the true solutions. The appearance of such degeneracies is due to both the inherent three flavour structure of the oscillation probabilities, and some still unknown neutrino oscillation parameters. The presence of the latter degeneracies in the analysis of a beta-beam experiment depends on our knowledge of neutrino oscillation properties at the time such measurement is performed. These degeneracies are of four different kinds, namely the intrinsic, the sign, the octant and the mixed degeneracies (or clones). The classification corresponds to the following origins:

- for an appearance experiment the oscillation probability Eq.(14) obtained for neutrinos at fixed baseline and energy has a continuous number of solutions (δ, θ_{13}). If the same experiment is performed for both neutrinos and anti-neutrinos with the same energy, only two disconnected solutions are left that satisfy the equation $P_{\alpha,\beta}^{\pm}(\delta, \theta_{13}) = P_{\alpha,\beta}^{\pm}(\bar{\delta}, \bar{\theta}_{13})$ (where $\pm$ refers to neutrino and anti-neutrino respectively). These two regions correspond to the true solution and the intrinsic clone (Burguet-Castell *et al* 2001).
- The sign of Δm_{23}^2 is still unknown. The positive and negative solutions give two different regions called the sign clones (Minakata and Nunokawa 2001).
- The two octants $\theta_{23} > \pi/4$ and $\theta_{23} < \pi/4$ are possible, giving in general two possible solutions for δ and θ_{13}. This is called the octant degeneracy (Fogli and Lisi 1996).
- A "wrong" sign and a "wrong" octant give rise to a new degeneracy called the mixed clone.

The ensemble of these four regions for the true solution and the intrinsic clone gives eight different solutions also called the eightfold degeneracy (Barger *et al* 2002). In (Donini *et al* 2004) it is pointed out that the clone solutions can be significantly different if determined from the oscillation probability, or from the number of events, showing that the degenerate solutions should be computed from the number of events, which is the physically measured quantity. Analytical formulae to determine the clone locations as a function of the real solutions are given. The effect of possible combination of super-beams and beta-beams (Section II) as well as of a neutrino factory with super-beams and/or beta-beams is discussed. A detailed analysis of the eightfold degeneracy is performed for the first time in (Donini *et al* 2005b). It is shown that combining
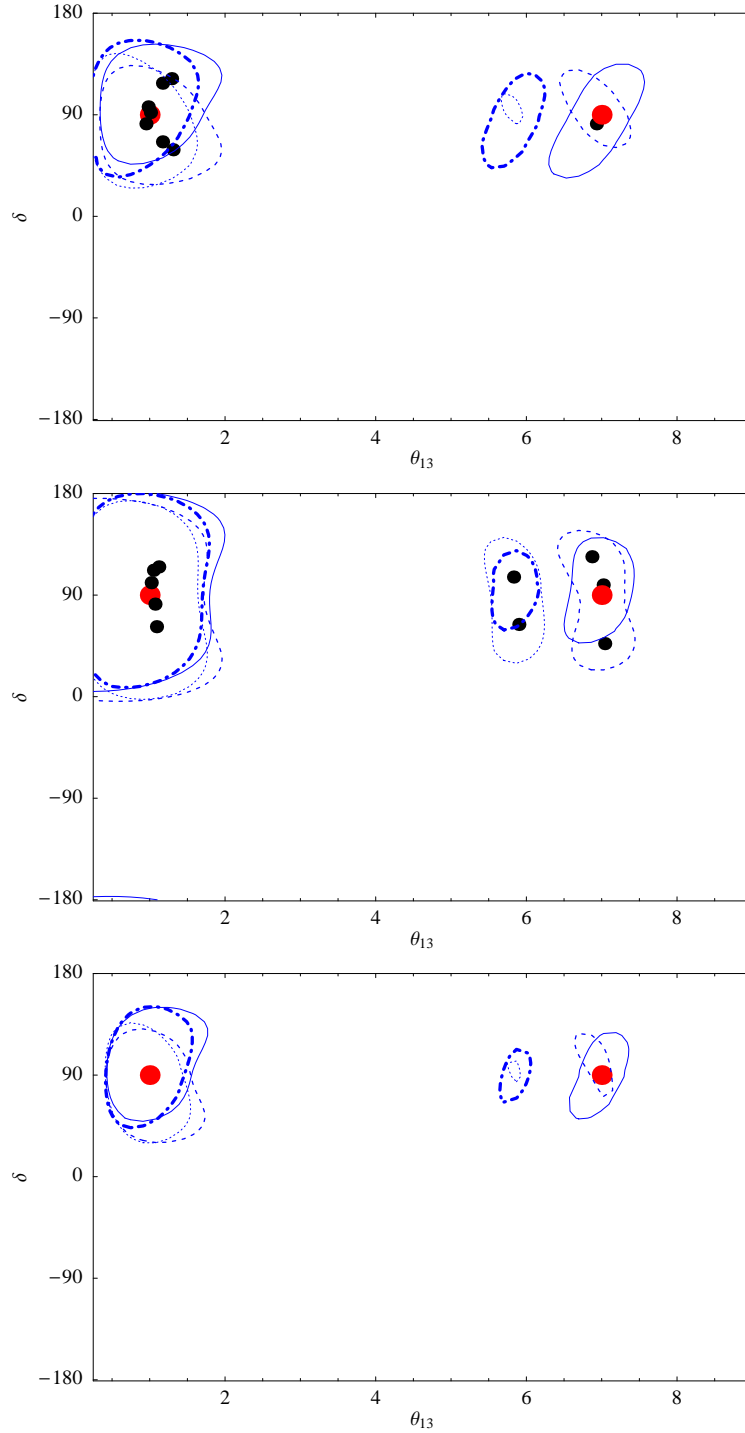
Figure 27. The figure shows the 90% CL contours for $\theta_{13} = 1°, 7°$ and $\delta = 90°$ (light red circle), after a 10 year β-Beam (upper), a 2+8 year Super-Beam (middle) and a combined measurement (lower figure). The different clone regions are shown (see text): the intrinsic (solid), the sign (dashed), the octant (dot-dashed) and the mixed (dotted line) degeneracies. The theoretical clone locations are presented as well (dark black dots) (Donini *et al* 2005b).
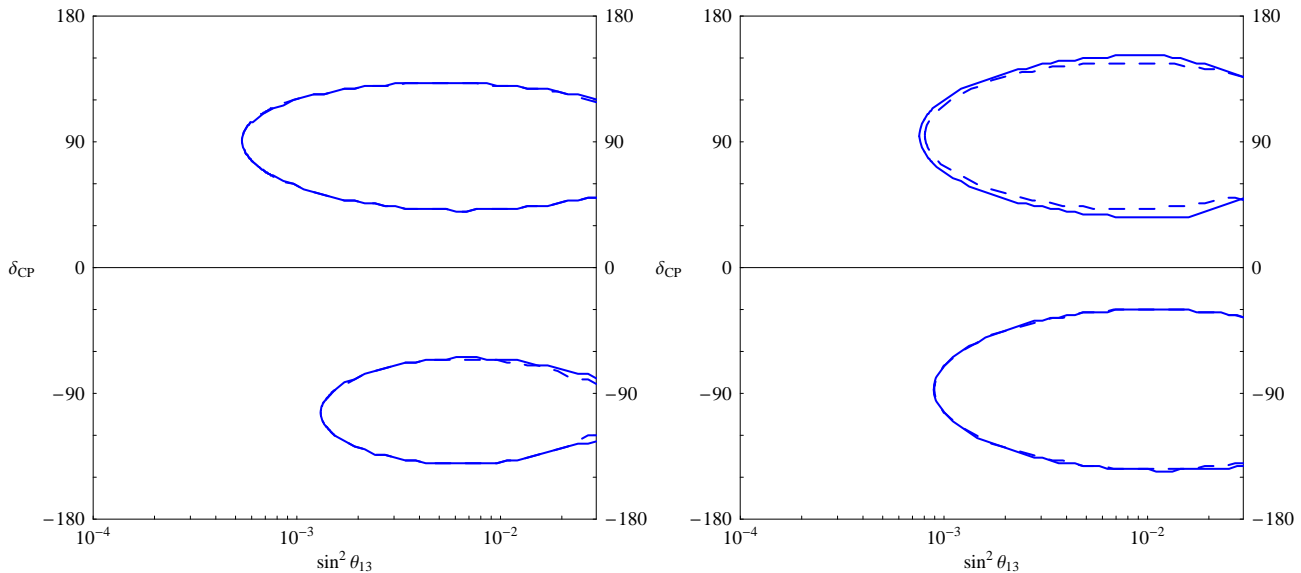
Figure 28. CP discovery potential in the (θ_{13}, δ) plane at 99 % C.L. for a super-beam (left) and a beta-beam (right), considering the appearance channel only (dashed line), and a combination of the appearance and the disappearance channels (solid line) at the same facility. A 2% systematic error in the disappearance channel and a 5% systematic error in the appearance channel have been considered for both facilities (Donini *et al* 2005c).

a super-beam and a beta-beam does not solve the problem of degeneracies, since, at the neutrino energies involved, both are counting experiments, tuned at the same L/E value. Some clone regions are eventually reduced (Figure 27). Different strategies can be followed to resolve the degeneracy issue, such as the use of spectral analysis (Burguet-Castell *et al* 2001), combination of various experiments (Minakata *et al* 2003), and/of different channels (Donini *et al* 2002). In (Donini *et al* 2005c) the combination of the appearance and disappearance channels is explored both for the original beta-beam and for a super-beam, showing that while there is no improvement for the former as soon as some level of systematic error is added, degeneracies are reduced for the latter. Figure 28 presents the discovery potential for each of these options taken alone, taking fully into account the degeneracies. Note that the $\mathcal{CP}$ sensitivity contours have only an approximate symmetry for $|\delta| \geq \pi/2$ and $|\delta| \leq \pi/2$, while there is no symmetry between positive an negative values of δ. The impact of the degeneracies on the $\mathcal{CP}$ discovery reach for the $\gamma = 100$ option is also shown in Figure 29 (Campagne *et al* 2006). A discussion on the issue of degeneracies can be found in (Rigolin 2005a and 2005b) as well.

Recently a very interesting idea has been proposed to resolve the open problem of the degeneracies, namely to combine accelerator experiments with data from atmospheric neutrinos provided by the same detector (Huber *et al* 2005b). In fact atmospheric neutrinos are sensitive to θ_{13} and the mass hierarchy due to earth matter
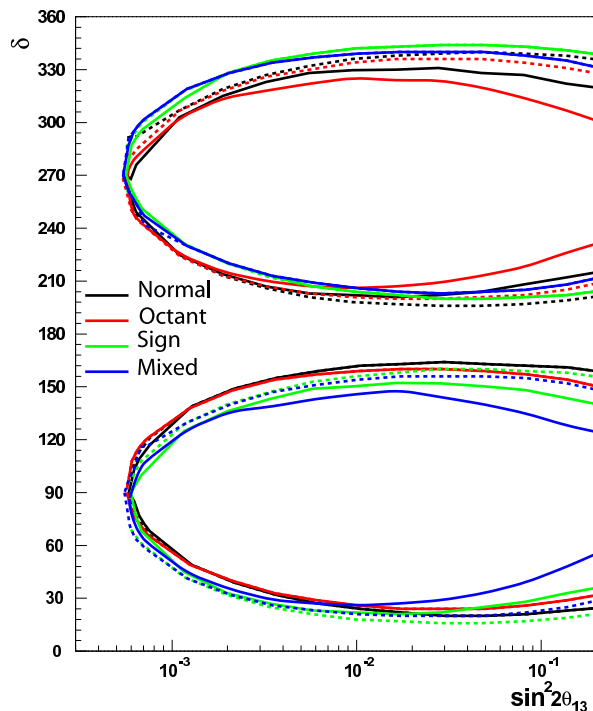
Figure 29. Impact of the degeneracies on the $\mathcal{CP}$ discovery potential for the $\gamma = 100$ beta-beam. We show the sensitivity at 3σ ($\Delta\chi^2 > 9$) computed for 4 different options about the true parameter values: Normal: $sign(\Delta m_{31}^2) = 1$, $\theta_{23} = 40°$; Octant: $sign(\Delta m_{31}^2) = 1$, $\theta_{23} = 60°$; Sign: $sign(\Delta m_{31}^2) = -1$, $\theta_{23} = 40°$; Mixed: $sign(\Delta m_{31}^2) = -1$, $\theta_{23} = 60°$. Dotted curves are computed neglecting degeneracies (Campagne *et al* 2006).

effects in the *e*-like events. In addition effects from the solar parameters and Δm_{12}^2 on *e*-like events in the sub-GeV energy range provide a sensitivity on θ_{23}. Due to these effects the sign and octant degeneracies can be broken. A first application is done in (Campagne *et al* 2006) which shows that the true solutions are identified by the combined accelerator and atmospheric data both for a beta-beam and a super-beam (SPL) at CERN (Figure 30). In particular, the hierarchy can be identified at 2σ C.L. from a combined analysis if $\sin^2\theta_{13} \geq 0.03 - 0.05$ for the beta-beam and the super-beam while the octant can be determined through the super-beam and the atmospheric data. Let us recall that these experiments alone have no sensitivity at all on the octant and sign issues. This important synergy between accelerator and atmospheric data is clearly very promising for the identification of the true value of the third mixing angle as well as of the $\mathcal{CP}$ violating phase in a beta-beam experiment.

6. Monochromatic neutrino beta-beams

An exciting variant to the original beta-beam idea has been proposed, where monochromatic neutrino beams are produced through the electron capture of radioactive ion beams (Bernabeu *et al* 2005a). The baseline of such a facility would be the same
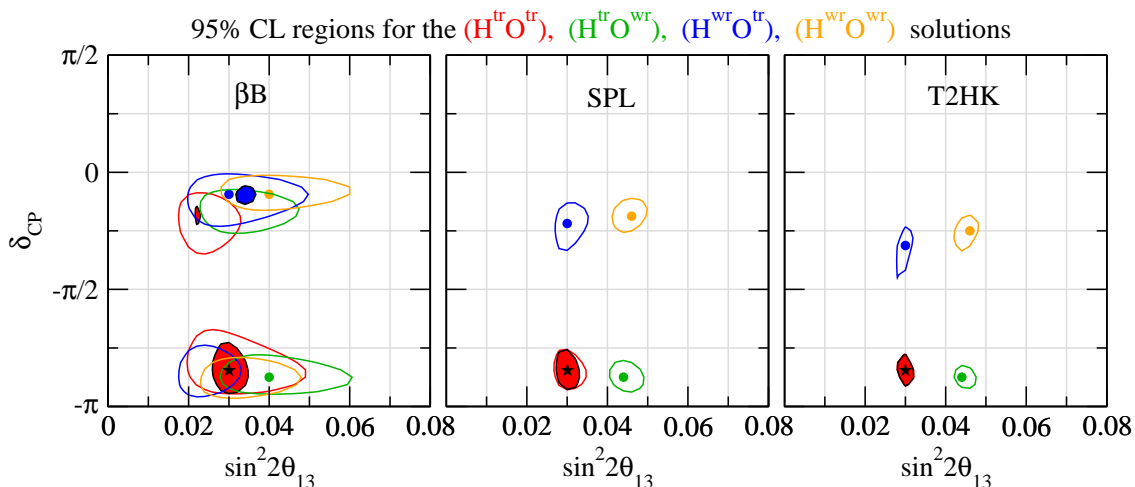
Figure 30. Impact on the degeneracies of a combined accelerator and atmospheric data analysis, in the case of a $\gamma = 100$ beta-beam and a super-beam (SPL) at CERN on one hand, and of T2K phase II to Hyper-K (Itow *et al* 2001) on the other hand. The figure shows the allowed regions in $\sin^2 2\theta_{13}$ and δ_{CP} for accelerator data alone (contour lines) and accelerator plus atmospheric data combined (colored regions). Solution for the true/wrong mass hierarchy (octant of θ_{23}) are indicated with $H^{tr/wr}(O^{tr/wr})$. The true parameter values are $\delta_{CP} = -0.85\pi$, $\sin^2 2\theta_{13} = 0.03$, $\sin^2 \theta_{23} = 0.6$ (Campagne *et al* 2006).

as for the original beta-beam facility (Zucchelli 2002) (Fig. 8). The production of such beams depends on the existence of ions decaying through electron capture with a short enough lifetime for electron capture to occur. In fact one needs to keep one electron bounded to the ion and therefore to produce, accelerate and store partly charged ions. Since, even in a very good vacuum conditions, a few remaining atoms make the ions quickly lose the electron, it is crucial that their lifetime is short enough to have high neutrino intensities. Good candidates are offered by some recently discovered nuclei far from the stability line, which have a fast decay through an allowed transition to a Gamow-Teller resonance in the energetically accessible region. Examples of such nuclei are given in Table 4. The monochromatic neutrino flux produced by electron capture and arriving in a detector at a given distance L is

$$\frac{d^2 N_\nu}{dS dE} \approx \frac{\Gamma_\nu N_{ions} \gamma^2}{\Gamma \pi L^2} \delta(E - 2\gamma E_0) \tag{22}$$

with $\gamma >> 1$, N_{ions} is the total number of decaying ions, Γ_ν/Γ is the branching ratio for electron capture (Table 4). The quantities E_0 and $E = E_0/[\gamma(1 - \beta \cos\theta)]$ represent the energy in the rest and in the laboratory frames respectively, with the angle θ being the deviation of the neutrino with respect to the prolongation of the long straight section of the decay ring.

There is a major difference in the use of neutrino beams coming from electron capture and from beta-beams in the search for $\mathcal{CP}$, since only electron neutrino beams can be produced in the first case. As a consequence, the study of $\mathcal{CP}$ violation cannot be made through a comparison of neutrino versus anti-neutrino oscillations Eq.(10), but by

Table 4. Decay properties of some rare-earth nuclei. The half-life and the branching ratios for electron-capture relative to beta-decay are given in the first columns, while the last column presents the neutrino energy in the rest frame, defined as the Q_β-value minus the energy at which the Gamow-Teller resonance is located (see text). The given ions are example candidates for a beta-beam facility producing monochromatic beams through electron capture (Bernabeu *et al* 2005a).

Decay	$t_{1/2}$	EC/β_+ (%)	E_0(keV)
^{148}Dy $\rightarrow^{148}$Tb	3.1 m	96/4	2062
^{150}Dy $\rightarrow^{150}$Tb	7.2 m	99.9/0.1	1397
^{152}Tm $2^- \rightarrow^{152}$Er	8.0 s	45/55	4400
^{150}Ho $2^- \rightarrow^{150}$Dy	72 s	77/33	3000

performing oscillation measurements at different ion boosts. In fact, for a fixed distance between the source and the detector, the appearance probability for $\nu_e \rightarrow \nu_\mu$ being energy dependent, the effect of the δ phase is to shift the oscillation interference pattern, while the amplitude of the oscillation probability is determined by the mixing angle θ_{13} (Figure 31) (Bernabeu *et al* 2005a). As a consequence the values of these unknown parameters can be extracted by comparing the $\nu_e \rightarrow \nu_\mu$ oscillation probability at different neutrino energies (ion boosts). Note that since the energy of the monochromatic neutrino beams can be well determined, such an energy dependent measurement does not need any energy reconstruction in the detector. The main advantage of the electron capture case over beta-beams is that in the former case the energy of all neutrinos can be peaked at the energy(ies) of interest, to match the the oscillation maxima; while in the latter case, because of the broad spectrum (Fig.6), for a given intensity, many neutrinos will be in an energy range which is less sensitive to the phase and/or where the cross section is low.

The sensitivity to $\mathcal{CP}$ violation has been studied in (Bernabeu *et al* 2005a), also in combination with a β^-−beam (Bernabeu *et al* 2005b). Figure 32 shows the sensitivity in the (δ, θ_{13}) plane for four chosen values of these parameters. The source is of 10^{18} ^{150}Dy ions/year, for a running time period of 10 years. The ions run 5 years at the Lorentz boost $\gamma = 195$ - the maximum achievable at the CERN's SPS (Fig.8) - and 5 years at $\gamma = 90$, chosen to be as different as possible from the first one and high enough to avoid backgrounds. The water Čerenkov detector has 440 kton fiducial mass and is located at a distance of 130 km (the CERN-Fréjus distance).

The possibility of using monochromatic electron neutrino beams to perform $\mathcal{CP}$ violation searches appears very promising. A detailed study concerning the ion production rates, the target and ion source design, the accumulation scheme as well as possible vacuum improvements is now required, to definitely state the achievable flux.
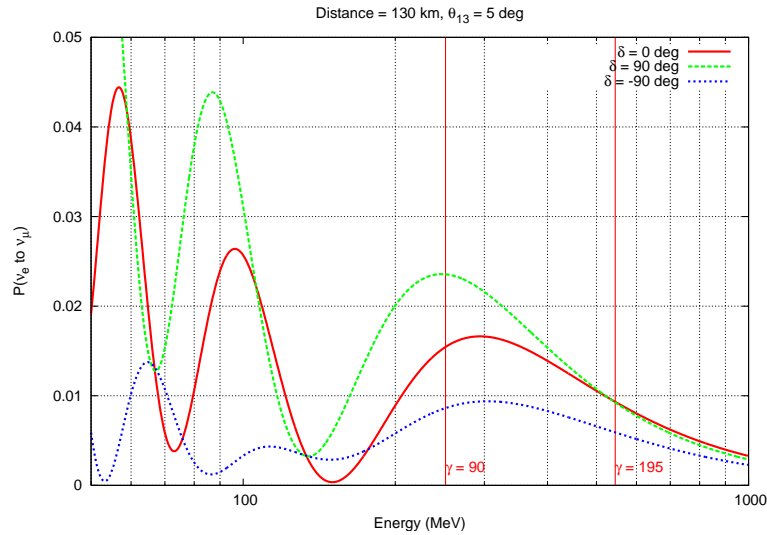
Figure 31. Appearance probability for neutrino oscillations in the three flavour formalism and a non-zero Dirac δ phase, as a function of neutrino energy, with a distance between the source and the detector of 130 km. The three curves correspond to three different values of the phase δ, while the vertical lines show the two ion Lorentz boosts used in the simulation (Bernabeu *et al* 2005a) .
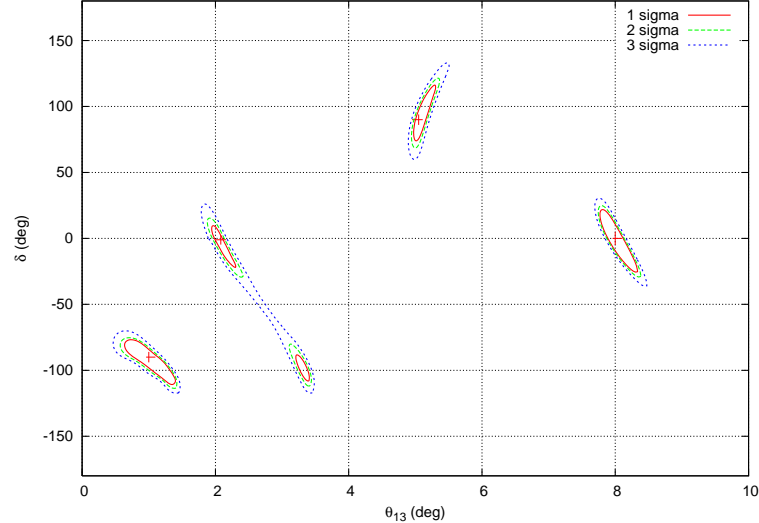

Figure 32. Sensitivity to the $\mathcal{CP}$ violating phase δ and the still unknown mixing angle θ_{13}. The results are obtained considering neutrino beams from electron-capture of partly charged ^{150}Dy ions, boosted at $\gamma = 90, 195$. The different curves show the confidence levels for the assumed values $(8°, 0), (5°, 90°), (2°, 0)$ and $(1°, -90°)$. The details on the used setup can be found in the text (Bernabeu *et al* 2005a).

7. Conclusion and perspectives

The recent discoveries in the field of neutrino physics open important new developments. Some require in particular pure, intense and well controlled neutrino beams, such as

those furnished by "beta-beams". This novel method exploits the intense radioactive ion beams under study, and offers important synergies with the nuclear physics community. A new facility based on beta-beams has been proposed with the main goal of addressing the crucial issue of the existence of $\mathcal{CP}$ violation in the lepton sector. In the original scenario information on the $\mathcal{CP}$ violating phase is extracted from a comparison of neutrino versus anti-neutrino oscillations. The neutrino beams are produced at CERN, and sent to a gigantic Cerenkov detector located in the Fréjus Underground Laboratory, 130 km from CERN. The first steps of the facility are very similar to the EURISOL project, while the acceleration to GeV energies uses already existing accelerator infrastructures (the PS and SPS) which implies important savings in the cost. The ions are then stored in a large storage ring that needs to be built. This scenario has also the significant advantage that it uses reasonable extrapolation of existing technology.

While a beta-beam alone already has a very interesting discovery potential, it can be pushed even further if a very intense conventional beam is fired to the same detector as well. This combination also offers the possibility to perform studies of the $\mathcal{T}$ and $\mathcal{CPT}$ symmetries. On the other hand, it has recently been pointed out that if the $\mathcal{CPT}$ symmetry is assumed, the neutrino measurements with a beta-beam and a super-beam in the $\mathcal{T}$ channel can be used to reduce the measurement time from 10 to 5 years. The achieved sensitivity is very close to that of a single experiment running for 10 years in both the neutrino and the anti-neutrino modes.

The discovery reach of the original scenario is being explored in great detail. Various options are considered, such as running the neutrino and antineutrino emitters either together or independently in the storage ring, and/or varying the Lorentz ion boost from 60 to the maximum acceleration achievable in the SPS. (If at γ of about 60 the experiment is a counting experiment only, already at about 100 some information on the energy of the events can be exploited.) This facility is well positioned to explore values between 10^{-3} to 10^{-4} for the third still unknown neutrino mixing angle θ_{13}. For the $\gamma = 100$ option the maximal violation corresponding to $\delta = \pi/2$ and $3\pi/2$ can be discovered down to $\sin^2 2\theta_{13} = 6(8)\ 10^{-4}$ (99 % C.L.) for the beta-beam (super-beam); while the best sensitivity is obtained for $\sin^2 2\theta_{13} > 10^{-2}$ since at this value $\mathcal{CP}$ violation can be established for 73 % (75 %) for all δ values with a beta-beam (super-beam). The comparison with e.g. T2K phase II to Hyper-K in Japan – a project of similar size and timescale – shows a very similar discovery reach. Besides, the MEMPHYS detector has the same physics potential for proton decay and for (extra-)galactic supernova neutrinos as UNO in the US and Hyper-K.

A variant of the original beta-beam idea consists in using ions decaying through electron-capture instead of beta-decay. This option has the advantage that the neutrino beams are mono-chromatic. (No anti-neutrino beams can be produced.) Information on the δ phase is extracted in this case by performing experiments at different ion boosts, since the phase introduces shifts in the appearance oscillation patterns. The recent discovery of exotic nuclei that have fast decay through a strong Gamow-Teller

transitions offer good potential candidates for the neutrino emitters. The required baseline is here the same as in the original beta-beam scenario. A specific feasibility study is now required as far as the achievable intensities and vacuum issues are concerned for example, since not fully stripped ions need to be accelerated and stored. Also, the sensitivity studies are to be pushed further.

Medium and high energy scenarios have been proposed as well, where the ion boosts are of several hundreds and thousands respectively. Such energies require new baseline scenarios: new accelerator infrastructures, such as a refurbished SPS (for the medium energy case), or the LHC (for the high energy case); a much bigger storage ring to stack the ions; a longer source to detector distance, to match the first neutrino oscillation maximum. New sites for the far detector are to be identified like the Gran Sasso Underground Laboratory at about 700 km (for a boost of 350), or the Canfranc Underground Laboratory at 300 km (for γ=150). These scenarios benefit of increased statistics, of the energy dependence of the events and eventually of matter effects, with an enlarged discovery potential: an increased sensitivity; information on the still unknown neutrino mass hierarchy; a reduction of the degeneracies with a better identification of the true location of the unknown angle and of the phase. From the physics point of view these scenarios with $\gamma > 150$, and particularly the medium energy ones, are very promising. However, they keep, at least for the moment, at a more speculative level than the original one, since they are not based on existing accelerator complex, nor on a robust evaluation of the ion intensities. Clearly these options deserve further studies.

The analysis of a $\mathcal{CP}$ violating experiment will depend on the knowledge of all other neutrino oscillation parameters at the time it takes place. At the moment the unknown sign of Δm_{23}^2 and octant of θ_{23} introduce supplementary fake regions in the multidimensional oscillation parameter space besides those that correspond to the true solutions of θ_{13} and δ. A significant reduction of the degeneracies can be obtained in the medium and high energy options. On the other hand, the original beta-beam scenario has no sensitivity to the octant and to the sign issues, and is affected by degeneracies, even combined with a super-beam. The synergy of the accelerator measurements with atmospheric data in the same detector, as recently proposed, has been shown to be a very promising strategy to get rid of the clone solutions in this case as well. In particular, the hierarchy can be identified at 2σ C.L. from a combined analysis if $\sin^2 \theta_{13} \geq 0.03 - 0.05$ for the beta-beam and the super-beam, while the octant can be determined through the super-beam, thanks to the atmospheric data.

The establishment of a beta-beam facility is a natural site to have low energy beta-beams with neutrinos in the 100 MeV region. Such options open completely new possibilities besides $\mathcal{CP}$, $\mathcal{T}$, and $\mathcal{CPT}$ symmetries studies. The physics potential is being investigated. It covers different topics from nuclear structure and neutrino-nucleus to fundamental interaction studies as well as core-collapse Supernova physics. Since the neutrino flux emittance is low, a devoted storage ring appears as more appropriate for these applications.

In conclusion, a beta-beam facility has a rich and broad physics potential. The feasibility study of the original scenario, as well as of the small storage for low energy beta-beams, is now ongoing within the EURISOL Design Study. Both its outcome and future physics studies will furnish the necessary elements to assess the final discovery reach. The ongoing work has already shown that a beta-beam facility can clearly offer a very competitive strategy for future neutrino accelerator experiments, and much more.

References

Ahmad Q R [the SNO Collaboration] 2001 *Phys. Rev. Lett.* **87** 071301 [nucl-ex/0106015]

Ahn M H [the K2K Collaboration] 2003 *Phys. Rev. Lett.* **90** 041801 [hep-ex/0212007]

Agosteo *et al* 2002 *Nucl. Instr. and Meth. in Phys. Res.* B **194** 399

Agarwalla SK, Raychaudhuri A, Samanta A 2005 *Phys. Lett.* B **629** 33

Akimune H *et al* 1997 *Phys. Lett.* B **394** 23

Albright C *et al* 004 "The APS Neutrino Study" [physics/0411123]

ALEPH, DELPHI, L3, OPAL, and SLD Collaborations 2005 [hep-ex/0509008]

Angrik J *et al* [KATRIN Collaboration] 2004 "The KATRIN Design Report"

Anthony P L *et al* [SLAC E158 Collaboration] 2005 *Phys. Rev. Lett.* **95** 081601 [hep-ex/0504049]

Apollonio M *et al* [the CHOOZ Collaboration] 1999 *Phys. Lett.* B **466** 415 [hep-ex/9907037]

Ardellier *et al* 2004 [the Double CHOOZ Collaboration] [hep-ex/0405032]

Athanassopoulos C *et al* [LSND Collaboration] 1998 *Phys. Rev. Lett.* **81** 1774 [nucl-ex/9709006]

Athanassopoulos C *et al* [LSND Collaboration] 1996 *Phys. Rev. Lett.* **77** 3082 [nucl-ex/9605003]

Aunola M and Suhonen J 1996 *Nucl. Phys.* A **602** 133

Autin B *et al* 2003 *Jour. Phys.* G **29** 1785 [physics/0306106]

Avignone F T 2000 *et al Phys. Atom. Nucl.* **63** 1007 [physics/0306106]; see also http://www.phys.ornl.gov/orland

Balantekin A B, De Jesus J H, Volpe C 2006a *Phys. Lett.* B **634** [hep-ph/0512310]

Balantekin A B, De Jesus J H, Lazauskas R, Volpe C 2006b submitted [hep-ph/0603078]

Balantekin A B and Fuller G M 2003 *J. Phys.* G **29** 2513 [astro-ph/0309519]

Barger V, Marfatia D and Whisnant K 2002 *Phys. Rev.* D **65** 073023 [hep-ph/0112119]

Beacom J F and Vagins M R 2004 *Phys. Rev. Lett.* **93** 171101 [hep-ph/0309300]

Beacom J F and Vogel P 1999 *Phys. Rev. Lett.* **83** 5222 [hep-ph/9907383]

Beacom J F, Farr W M and Vogel P 2002 $\hat{P}$hys. Rev. D **66** 033001 [hep-ph/0205220]

Benedikt M, Hancock S, Lindroos M 2004 Proceedings to "EPAC 2004", Lucerne, Switzerland, 5-9 July

Benedikt M 2005 *Nucl. Phys. Proc. Suppl.* **149** 54, Proceedings to "NUFACT04", Osaka, Japan, 26 July, 1 August 2004

Benedikt M, Chancé A, Lindroos M, Payet J 2006 Private communication

Bennett S C and Wieman C E 1999 *Phys. Rev. Lett.* **82** 2484 [hep-ex/9903022]

Bernabeu J, Burguet-Castell J, Espinoza C, M. Lindroos M 2005a JHEP 0512 **014** [hep-ph/0505054]

Bernabeu J, Burguet-Castell J, Espinoza C, M. Lindroos M 2005b Proceedings to "NUFACT05", Frascati, Italy, 21-26 Jun 2005 [hep-ph/0510278]

Bernabeu J, Burguet-Castell J, Espinoza C 2005c Talk given at "EPS International Europhysics Conference on High Energy Physics (HEP-EPS 2005)", Lisbon, Portugal, 21-27 Jul 2005 [hep-ph/0512297]

Bernabeu J, Burguet-Castell J, Espinoza C, M. Lindroos M 2005d Proceedings to "GUSTAVOFEST: Symposium in Honor of Gustavo C. Branco: CP Violation and the Flavor Puzzle", Lisbon, Portugal, 19-20 Jul 2005 [hep-ph/0512299]

Bernabeu J *et al* 1988 IPNO/TH-88-58, FTUV-88/20

Bilenky S M, Giunti C, Grifols J A, Masso E 2003 *Phys. Rept.* **379** 69

Borzov I N and Goriely S 2000 *Phys. Rev. C* **62** 035501-1

Bouchez J, Lindroos M, Mezzetto M 2004 *AIP Conf. Proc.* **721** 37 [hep-ex/0310059]

Bouchez J 2005 *Nucl. Phys. Proc. Suppl.* **147** 93

Burguet-Castell J *et al* 2004 *Nucl. Phys.* B **695** 217 [hep-ph/0312068]

Burguet-Castell J *et al* 2005 *Nucl. Phys.* B **725** 306 [hep-ph/0503021]

Burguet-Castell J, Gavela M B, Gomez-Cadenas J J, Hernandez P ad Mena O 2001 *Nucl. Phys.* B **608** 301 [hep-ph/0103258]

Campagne J E, Maltoni M, Mezzetto M, Schwetz T 2006 [hep-ph/0603172]

Chancé A and Payet J 2005 Private communication

Christenson *et al* 1964 *Phys. Rev. Lett.* **13** L38

Daraktchieva Z *et al* [MUNU Collaboration] 2003 *Phys. Lett.* B **564** 190 [hep-ex/0304011]

Davidson S, Forte S, Gambino P, Rius N and Strumia A 2002 *JHEP* **0202** 037 [hep-ph/0112302]

Davis R 1964 *Phys. Rev. Lett.* **12**

Derbin A I *et al* 1993 *JETP Lett.* **57** 768

Deutsch J P, Macq P C and Van Elmbt L 1977 *Phys. Rev.* C **15** 1587

Diwan M V *et al* 2003 *Phys. Rev.* D **68** 012002 [hep-ph/0303081]

Donini A, Fernandez-Martinez E, Migliozzi P, Rigolin S, Scotto-Lavina L, Tabarelli de Fatis, Terranova 2005a *Nucl. Phys.* B **710** 402 [hep-ph/0511134]

Donini A, Fernandez-Martinez E, Migliozzi P, Rigolin S, Scotto-Lavina L 2005b *Nucl. Phys.* B **710** 402 [hep-ph/0406132]

Donini A, Fernandez-Martinez E, Rigolin S 2005c *Phys. Lett.* B **621** 276 [hep-ph/0411402]

Donini A, Meloni D, Rigolin S 2004 *JHEP* **0406** 011 [hep-ph/0312072]

Donini A, Meloni D and Migliozzi P 2002 *Nucl. Phys.* B **646** 321 [hep-ph/0206034]

Elliott S R and Engel J 2004 *J. Phys.* J **30** R183 [hep-ph/9604415]

Efremenko Y Private communication

Eguchi K *et al* [the KamLAND Collaboration] 2003 **90** *Phys. Rev. Lett.* 021802 [hep-ex/0212021]

Ereditato A and Rubbia A 2005 Proceedings to "NUFACT05", Frascati, Italy, 21-26 June [hep-ph/0510131]

Ereditato A and Rubbia A 2004 Proceedings to "HIF04", La Biondola, June [hep-ph/0412230]

The EURISOL Project, see http://ganinfo.in2p3.fr/eurisol/

Fogli G L and Lisi E 1996 *Phys. Rev.* D **54** 3667 [hep-ph/9604415]

Fogli G L, Lisi E, Mirizzi A, Montanino D 2005 *JCAP* **0504** 002

Fukuda *et al* [the Super-Kamiokande Collaboration] 1998 *Phys. Rev. Lett.* **81** 1562 [hep-ex/9807003]

GSI see http://www.gsi.de

Guglielmi A, Mezzetto M, Migliozzi P, Terranova F 2005 "The High Energy Frontier" [hep-ph/0508034]

Gomez-Cadenas JJ 2005 *Nucl. Phys. Proc. Suppl.* **145** 161

Giunti C and Laveder M 2002 [hep-ph/0202152]

Hancock S, Benedikt M, Vallet J-L 2003 CERN note AB-Note-2003-080 MD

Hardy J C and Towner I S 2005 P̂hys. Rev. C **71** 055501 [nucl-th/0412056]

Haxton W C 2004 Talk presented at "The r-process: The astrophysical origin of the heavy elements" [nucl-th/0406012]

Haxton W C, Langanke K, Qian Y Z, Vogel P 1997 *Phys. Rev. Lett.* **78** 2694 [astro-ph/9612047]

Huber P, Lindner M, Rolinec M, Winter W 2006 *Phys. Rev. D* **73** 053002 [hep-ph/0506237]

Huber P, Lindner M, Winter W 2005a *Comput. Phys. Commun.* **167** 195 [hep-ph/0407333]

Huber P, Maltoni M and Schwetz T 2005b *Phys. Rev.* D **71** [hep-ph/0501037]

Itow Y *et al* 2001 [hep-ex/0106019]

Jachowicz N and McLaughlin G C 2005 Proceedings of the "Erice International School of Nuclear Physics", Erice, Italy 16-24 September [nucl-th/0511069]

Jachowicz N and McLaughlin G C 2006 submittted

Jardin P *et al* 2002 *Rev. Sci. Instrum.* **73** 789

Jung C K 2000 [hep-ex/0005046]

Kneller J P, McLaughlin G C and Surman R 2004 [astro-ph/0410397]

Kolbe E and Langanke K 1999 *Phys. Rev.* C **60** 052801 [nucl-th/9905001]

Kortelainen M and Suhonen J 2002 *Europhys. Lett.* **58** 666

Kortelainen M and Suhonen J 2004 *Phys. Atom. Nucl.* **67** 1202

Kubodera K and Nozawa S 1994 *Int. J. Mod. Phys.* E **3** 101, and references therein

Langanke K and Martinez-Pinedo G 2004 *Nucl. Phys.* A **731** 365

Lee Y K, Mo L W and Wu C S 1963 *Phys. Rev. Lett.* **10** 253

Lee T D and Wu C S 1965 *Ann. Rev. Nucl. Sci.* **15** 381

Li H B *et al* [TEXONO Collaboration] 2003 *Phys. Rev. Lett.* **90** 131802

Lindroos M 2003 CERN-AB-2004-006-OP [physics/0312042]

Lindroos M and Volpe C 2004 *Nucl. Phys. News* **14** 15

Lindroos M 2005 EURISOL DS/TASK12/TN-05-02

Loinaz W *et al* 2004 *Phys. Rev. D* **70** 113004 [hep-ph/0403306]

Magistris M and Silari M note CERN-TIS-2003-017-RP-TN

Maki Z, Nakagawa M, Sakata S 1962 *Prog. Theor. Phys.* **28** 870

McLaughlin G C and Volpe C 2004 *Phys. Lett.* B **591** 229 [hep-ph/0312156]

McLaughlin G C 2004 *Phys. Rev.* C **70** 045804 [nucl-th/0404002]

McLaughlin G C and Fuller G M 1995 *Astrophys. J.* **455** 202

Meyer B S, McLaughlin G C and Fuller G M 1998 *Phys. Rev. C* **58** 3696 [astro-ph/9809242]

Mezzetto M *et al* 2003 *Jour. Phys.* G **29** 1771 [hep-ex/0302007]

Mezzetto M 2005a *Nucl. Phys. Proc. Suppl.* **149** 179

Mezzetto M 2005b Proceedings to "NUFACT05", Frascati, Italy, 21-26 June [hep-ex/0511005]

Miller G A and Thomas A W 2005 *Int. J. Mod. Phys.* A **20** 95 [hep-ex/0204007]

Migliozzi P 2005 *Nucl. Phys. Proc. Suppl.* **145** 199

Migliozzi P and Terranova F 2003 *Phys. Lett.* B **563** 73 [hep-ph/0302274]

Mikheev S P and Smirnov A Y 1986 *Nuovo Cimento* C **9** 17

Minakata H and Nunokawa H 2001 *JHEP* **0110** 001 [hep-ph/0108085]

Minakata H, Nunokawa H, Parke S J 2003 *Phys. Rev.* D **68** 013010 [hep-ph/0301210]

Mosca L 2005a *Nucl. Phys. Proc. Suppl.* **138** 203

Mosca L 2005b *Nucl. Phys. Proc. Suppl.* **138** 421

Muto K, Bender E and Klapdor H V 1989 *Z. Phys.* A **334** 177

Osterfeld F 1992 *Rev. Mod. Phys.* **64** 491

Pontecorvo B 1957 *Sov. Phys. JETP* **6** 429

Qian Y Z *et al* 1997 *Phys. Rev. C* 1532

Raffelt G G 1996 *Stars As Laboratories For Fundamental Physics: The Astrophysics Of Neutrinos, Axions, And Other Weakly Interacting Particles*, Chicago, USA: Univ. Pr.; and references therein

Reines F, Gurr H S and Sobel H W 1976 *Phys. Rev. Lett.* **37** 315

Rigolin S 2005a *Nucl. Phys. Proc. Suppl.* **145** 203

Rigolin S 2005b Proceedings to "NUFACT05", Frascati, Italy, 21-26 June [hep-ph/0509366]

Rodin *et al* 2003 *Phys. Rev.* C **68** 044302, and references therein

Rubbia C 1977 CERN-EP/77-08

Rubbia A 2004 Proceedings to "HIF04", La Biondola, June [hep-ph/0412230]

Ruffert M, Janka H T, Takahashi K and Schafer G 1997 *Astron. Astrophys.* **319** 122 [astro-ph/9606181]

Serreau J and Volpe C 2004 *Phys. Rev.* C **70** 055502 [hep-ph/0403293]

Singh SK, Sajjad Athar M, Ahmad S [nucl-th/0603001]

Sortais P 2003 Talk given at the Moriond workshop "Radioactive beams for nuclear physics and neutrino physics", Les Arcs

Terasawa M *et al* 2004 *Astrophys. J.* **608** 470

Terranova F, Marotta A, Migliozzi P, Spinetti M 2004 *Eur. Phys. J.* C **38** 69

Terranova F 2005 *Nucl. Phys. Proc. Suppl.* **149** 185, Proceedings to "NUFACT04", Osaka, Japan, 26 July, 1 August 2004

Thomas A W 1996 [nucl-th/9609052]

Vidyakin G S *et al* 1992 *JETP Lett.* **55** 206

Vogel P and Beacom J F 1999 *Phys. Rev.* D **60** 053003 [hep-ph/9903554]

Vogel P and Engel J 1989 *Phys. Rev.* D **39** 3378

Volpe C 2004 *Jour. Phys.* G **30** L1 [hep-ph/0303222]

Volpe C 2005a *Jour. Phys.* G **31** 903 [hep-ph/0501233]

Volpe C 2005b *Nucl. Phys.* A **752** 38 [hep-ph/0409357]

Volpe C 2005c *Nucl. Phys. Proc. Suppl.* **143** 43 [hep-ph/0409249], and references therein

Volpe C 2006 *Nucl. Phys. Proc. Suppl.* B **155** 97 [hep-ph/0510242]

Volpe *et al* 2000 *Phys. Rev. C* **62** 015501 [nucl-th/0001050]

Volpe *et al* 2002 *Phys. Rev. C* **65** 044603 [nucl-th/0103039]

Weinberg S 1958 *Phys. Rev.* **112** 1375

Wenander F *et al* 2003, to be published in RSI

Wilkinson D H 2000 *Eur. Phys. J.* A **7** 307

Winter W 2006 [hep-ph/0603012]

Wolfenstein L 1978 *Phys. Rev. D* **17** 2369

Woosley S E *et al* 1990 *Astrophys. J.* **356** 272

Wu C S 1964 *Rev. Mod. Phys.* **36** 618

Zeller G P *et al* [NuTeV Collaboration] 2002 *Phys. Rev. Lett.* **88** 091802 [Erratum-ibid. **90** (2003) 239902] [hep-ex/0110059]

Zucchelli P 2002 *Phys. Lett.* B **532** 166